AMINO ACID CONJUGATED SELF ASSEMBLY MOLECULES MODIFIED SI WAFERS

by

BENGÜ AKTAŞ

B.S., Biochemistry, Ege University, 2011

Submitted to the Institute of Biomedical Engineering
in partial fulfillment of the requirements
for the degree of
Master of Science
in
Biomedical Science

Boğaziçi University
2014

AMINO ACID CONJUGATED SELF ASSEMBLY MOLECULES MODIFIED SI WAFERS

APPROVED BY:

Assist. Prof. Dr. Bora Garipcan .....
(Thesis Advisor)

Assoc. Prof. Dr. Albert Güveniş .....

Assist. Prof. Dr. Sedat Odabaş .....

DATE OF APPROVAL: 14 August 2014

ACKNOWLEDGMENTS

I would like to express my appreciation and special thanks to my advisor Asist. Prof. Dr. Bora Garipcan for continuous support of my M.Sc research and for his patience and immense knowledge. I would also like to thank to my committee members, Assoc. Prof. Dr. Albert Güveniş and Assist. Prof. Dr. Sedat Odabaş for their encouragement and insightful comments.

In addition, I would like to give special thanks to my family for the support they provided me through my entire life. Words cannot express how grateful I am to my mother, my father and my brother for all of the sacrifices that they've made on my behalf.

Furthermore, I would like to thank my friends, Ayşegül Tümer, Agah Karakuzu, Öznur Demir, Selin Yalvarmış, Özgen Öztürk, Samet Kocatürk, Elif Dönmez, and Onur Arslan who supported me in every stage of this thesis. In the end, I would also give my thanks to my laboratory colleagues for exchanging knowledge and for all the fun we have had.

This thesis was supported by grants from TÜBİTAK project (112T564) and Bogazici University BAP Coordination Office.

ABSTRACT

AMINO ACID CONJUGATED SELF ASSEMBLY MOLECULES MODIFIED SI WAFERS

In this thesis, Si wafer surface was modified with newly synthesized self-assembled monolayers to mimic a biocompatible micro-environment for the cells and to observe their behavior. Begin with; Si wafer is chosen as its availability is easy and well-established structures can be obtained in the surface modification without any interference. In the first step, Si wafers were cleaned and modification of surfaces was carried out with amino acid conjugated self-assembled molecules [Histidine-Self Assembled Molecule (His-SAM), and Leucine-Self Assembled Molecule (Leu-SAM)], (3-aminopropyl)triethoxysilane (APTES) and also poly-L-ornithine (PLO). The characterization of these samples were analyzed with contact angle measurements, X-Ray Photoelectron Spectroscopy (XPS), Atomic Force Microscopy (AFM), and ellipsometry. After characterization results were acquired, the cell culture studies were performed with L929 cells. In order to obtain information about cell proliferation, MTT assay (a colorimetric assay) was performed. According to these results, enhanced cell proliferation was achieved by the contribution of surface functional groups. Consequently, it has been observed that these controlled molecular structures on the surfaces of materials have a great potential for biomedical applications.

Keywords: Silicon Wafer, Surface Modification, Self-assembled Molecules (SAMs), Amino Acids.

ÖZET

AMİNO ASİT KONJUGE KENDİLİĞİNDEN DÜZENLENEN MOLEKÜLLER İLE Sİ PULCUKLARIN MODİFİKASYONU

Bu tez çalışmasında, Si pulcuk yüzeyine sentezi yeni gerçekleştirilen amino asit konjuge kendiliğinden düzenlenen moleküller ile yüzey modifikasyonu yapılarak hücreler için biyouyumlu mikro-çevre taklit edilmiş ve bu yapıya hücrelerin tepkisi incelenmiştir. Başlangıçta, kullanılabilirliği basit olan ve kolay yapılandırılabilir bir malzeme olduğu için yüzeyde hiçbir girişim gerçekleşmeden modifikasyon yapılabilen Si pulcuklar substrat olarak seçilmiştir. İlk aşamada, Si pulcukların yüzeyleri temizlenmiş, amino asit konjuge kendiliğinden düzenlenen moleküller [Histidin-Kendiliğinden Düzenlenen Molekül (His-KDM) ve Lözin-Kendiliğinden Düzenlenen Molekül (Löz-KDM)], 3-Aminopropiltrietoksilan (APTES) ve poli-L-ornithin (PLO) ile yüzey modifikasyonu gerçekleştirilmiştir. Daha sonra yüzeylerin karakterizasyonu temas açısı ölçümleri, X-ışını fotoelektron spektroskopisi, atomik güç mikroskobu ve elipsometri ile analiz edilmiştir. Karakterizasyon sonuçları elde edildikten sonra L929 fibroblast hücreleriyle hücre çalışmaları gerçekleştirilmiştir. Hücre çoğalması hakkında bilgi sahibi olmak için MTT analiz yöntemi gerçekleştirilmiştir. Bu sonuçlara göre, yüzeyde bulunan fonksiyonel grupların katkısıyla artan hücre çoğalımının gerçekleştiği görülmüştür. Sonuç olarak, malzeme yüzeylerinde kontrollü oluşturulan molekül yapıların biyomedikal uygulamalar için büyük potansiyele sahip olduğu gözlenmiştir.

Anahtar Sözcükler: Si Pulcuk, Yüzey Modifikasyonu, Kendiliğinden Düzenlenen Moleküller (KDM ler), Amino Asitler.

TABLE OF CONTENTS

LIST OF FIGURES

LIST OF TABLES

LIST OF SYMBOLS

θ	Contanct Angle

LIST OF ABBREVIATIONS

Si	Silicon
SAM	Self Assembled Molecule
His-SAM	Histidine Self Assembled Molecule
Leu-SAM	Leucine Self Assembled Molecule
APTES	(3-Aminopropyl)triethoxysilane
PLO	Poly-L-Ornithine
XPS	X-Ray Photoelectron Spectroscopy
^{1}H-NMR	Proton Nuclear Magnetic Resonance
FTIR	Fourier Transform Infrared Spectroscopy
SEM	Scanning Electron Microscopy
ECM	Extracellular Matrix
DMSO	Dimethyl Sulfoxide
Cbz-AA-Bt	Carbobenzyloxy Amino Acid Benzotriazole
PBS	Phosphate Buffer Saline
DMEM	Dulbeccoâs Modified Eagle Medium
MTT	3-(4,5-dimethylthiazol-2-yl)-2,5-diphenyltetrazolium bromide
CVD	Chemical Vapour Deposition
PVD	Physical Vapour Deposition
PECVD	Plasma Enhanced Chemical Vapour Deposition

1. INTRODUCTION

1.1 Motivation

The development of biological materials has recently made great progress in tissue repairing and creating artificial organs. In the beginning, the materials have been merely designed according to their mechanical properties that include being inert and preventing any rejection in the body. By including biological and chemical improvements over materials such as bioactive components or biomimetic components from synthetic materials, new methods have been developed such as self-assembling method [1]. Thus, the new materials which are at the molecular level have gain an insight and surface engineering has become a more important area in the biomedical applications.

Materials allow communication with living cells and their environment through their interfaces. Furthermore, chemistry and physical topography of the surfaces play an important role in the cells behavior such as differentiation, adhesion, viability and proliferation [2, 3]. Therefore, scientists focused their attention to microscale and nanoscale approaches which in return made the top-down processing one of the famous studies in tissue and surface engineering [4]. For achieving these approaches, the criteria like synthesis, design and fabrication of biomaterials at molecular level were taken into consideration. New self-assembling procedures are also included in the fabrication of these biomaterials for years [2].

Self-assembled structures can be found in many systems ranging from microscale to macroscale, especially in living cells. That is why; it is one of the most studied topics in many areas such as drug release systems, sensory systems, surface modifications etc.[5]. For studying with cells, it is possible to create new surfaces with specific substrates such as amino acids, peptides, sugars or ECM proteins with the method of self-assembly [6]. Self-assembly is described as organization of disordered components without any external intervention [5]. These molecules undergo formation with non-covalent bonds such as ionic bonds, hydrogen bonds, and hydrophobic interactions etc. [3].

In recent years, self-assembled monolayers have become very popular because of the ease of the application of their formation procedure and their affinities for materials and they have been used in many cell studies [7]. Their functional groups provide the control of properties of materials, hence the environments and the cells. Although, it is still not clear how cells perceive the characteristic of the environment and translate the information into signals by the aid of protein, studies show that the properties such as surface roughness, type and distribution of functional groups and presence of hydrophilic-hydrophobic groups in the surface may contribute to cellular responses which include attachment, growth, proliferation and etc. [8, 9]. Therefore, different functional groups on self-assembled monolayers may affect the behavior of different cells by stimulating their receptors or changing the surface properties.

Based on this information, cell behavior may be controlled by newly synthesized different type of self-assembled monolayers and changing their parameters. Hence, highly biocompatible materials can be improved for a long term usage.

1.2 Objectives

In this study, Si wafer was used as a substrate since it has non-cytotoxic effect and well-established structures can be obtained in surface modification without any interference. Substrate was modified with newly synthesized amino acid conjugated self-assembled molecules to mimic micro-environment of L929 fibroblast cells. The main objectives of this study are:

- To form self- assembled monolayers with newly synthesized molecules,
- To investigate the effect of the surface modification of hydrophilic and hydrophobic amino acids and proteins as a medium substances on the cell behavior,
- To evaluate biocompatibility of surface modified silicon wafers.

1.3 Outline

This thesis is presented as follows: In chapter 2, background information about self-assembled monolayers, surface modification, surface engineering and cell behavior on substrate is given. In chapter 3, the experimental procedures are explained. In chapter 4, the results are presented. In chapter 5, the discussion of the results is given.

2. BACKGROUND

Biomaterials encompass the application of natural and synthetic materials to biological systems. It is an interdisciplinary area that includes biology, chemistry, physics, material science, and also engineering principles. Besides biomaterials comprise the medical applications; it is used in clinical analysis such as in fields of biochemistry and biotechnology for diagnostic purposes which includes the assay of blood proteins or gene array studies [10].

Biomaterials have widespread clinical use in reconstructive, cardiovascular, orthopedic and dental applications and other applications in which they are composed of a lot of materials ranging from ceramics, metals, and composites to new alloys [10], [11, 12]. However, some conditions should be taken into consideration while performing these applications and a more important one is known as a "host response". In order to overcome of host interaction problem and discard old traditional materials, scientists have developed new techniques since materials have a close association with living tissues. They suggested that bioactive nature of materials would have a positive effect on living organism so biological interactions between those materials and living tissue became the subject of great interest [12, 13, 14]. In order to understand this relationship, surface and tissue engineering fields have become focal points of the field of biomaterials.

2.1 Surface Engineering

Surface is a topological space which has properties such as having accessibility of molecules on it therefore allowing any kind of chemical reactions with external molecules. In parallel with, surface science which emerged from physics and chemistry enables one to determine molecule mechanism of structure and its properties, also to understand the dynamics and interfaces of reactions between other molecules. On the

basis of this information, surface science encompasses many concepts in it such as synthetic catalysis, semiconductors, adhesives, surface coatings etc. Therefore, many closely related areas also arose from this field such as surface engineering [11], [15].

Electronic, biomedical, petrochemical, textile, aerospace etc. are fields that surface engineering applications are widely used. Surface engineering in biomedical applications somewhat has a controversial history. The first studies had started in the 19th century; however the great progress has been made in the last quarter of this century [14].

Biological surface engineering provides an increase of the biocompatibility of material by modifying its surface while retaining the bulk material. The modification can be done by direct coating the surface or by changing atoms, molecules or compounds of surface physically or chemically [16].

Surfaces and interfaces of materials have an important role in the formation of biological reactions since there is a dynamic process between them. Biological system has a power called 'recognition system' which distinguishes foreign materials from their physical shape, chemical characteristics and topographies [17]. Initially, the material contacts with body fluid then blood proteins, hydrated ions and water surround the solid material. Water interactions lead to protein interactions with material. However, in 1987 Thiel and Madel, also in 2002 Henderson stated that dissociative adsorption of water can also occur in the surface [18], [19]. Correspondingly, the entire surface does not become in hydrophilic state. Therefore amino acids, peptide, proteins and other molecules with hydrophilic, hydrophobic, amphiphilic characters will interact with different domains of surface. After this stage, different type of cells reacts with related biomolecules at the surface (Figure 2.1.) [17], [20].

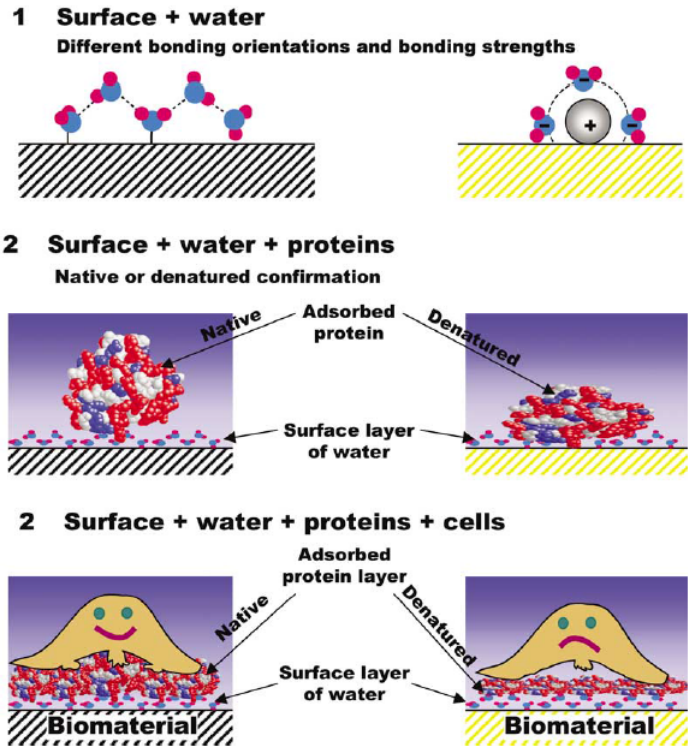

Figure 2.1 Molecule and cell interactions after implantation [20].

These interactions may affect perturbed tissue in a positive way in time. However, different interactions would cause adhesion problems on the surface. Also, undesirable interactions can influence the natural environment of living system [17], [20].

For these reasons, surface engineering is an important tool to design specific surfaces to establish desirable interactions with biological environments. There are two general methods for surface engineering; surface coatings and surface modifications [21].

Surface coating method comprises reinforcing the surface of the material by accumulating a layer of molten, semi-molten or chemical material. This process includes such techniques;

- Thin Film Coatings [20], [21], [22];
  - Chemical Vapour Deposition (CVD),
  - Physical Vapour Deposition (PVD),
  - Plasma Enhanced Chemical Vapour Deposition (PECVD).

- Plasma and thermal spraying [20], [23],
- Sol-gel [22],
- Cladding [22],
- Electroplating etc. [22].

Surface modification is performed because of improving physiochemical and topographical properties of materials. Modification enables materials to stabilize friction, wear and corrosion resistance features. Modification methods can be divided into subgroups such as induction, hardening by flame, laser or electron beam, high energy treatments. Here are the techniques in these groups;

- Wet chemical techniques [20];
  - Self-assembled monolayers,
  - Micro emulsions,
  - Colloidal chemistry,
- Nano- and microfabrication techniques [16], [21], [24];
  - Photolithography,
  - Soft lithograpy (micro-contact printing),
  - Ion beam implantation etc.
- Silanization and Langmuir-Blodgett Deposition [16],
- Immobilization of biomolecules [16],
- Texturing etc. [16].

Additionally, surface modification and coating methods can be applied together to achieve specific surfaces such as laser cladding.

After modification, surfaces should be analyzed in order to determine whether

modification can be made. There are many surface analysis methods such as surface spectroscopies to determine the composition of surface layer and, chemical and electronic state of elements such as X-Ray Photoelectron Spectroscopy (XPS), Secondary Ion Mass Spectroscopy (SIMS), Auger Electron Spectroscopy (AES) etc.; scanning probe techniques such as Scanning Tunneling Microscopy (STM) and Atomic Force Microscopy (AFM) for imaging surfaces at the atomic level; and Nuclear Magnetic Resonance Spectroscopy (NMR) and Electron Spin Resonance Spectrometer (ESR) to determine the chemical and physical properties of atoms and molecules by magnetic properties of atomic nuclei; Fourier Transform Infrared Spectroscopy (FTIR) and Sum Frequency Generation Spectroscopy (SFG) to specify the orientation distribution, and the composition of the surface; Ellipsometry to characterize roughness, thickness, and the composition of surface; and etc. [17], [20].

2.2 Self-Assembled Monolayers (SAMs)

Self-assembled monolayers (SAMs) are surfactant molecules which are ordered molecules including organic molecules and formed by spontaneous adsorption to the surface [25], [26]. SAMs can arrange physico-chemical properties such as type and density of functional groups, solvent interactions, adhesion, corrosion and wetting of organic interfaces. This method contributes to specific interactions and design flexibility [25], [27]. By using self-assembly method, molecules can be oriented and spaced with precision by the aid of surface energy minimization [14].

Normally, organic surfaces are less stable and less ordered and also more sensitive than inorganic surfaces. However, type of chemistry, the specific affinities of functional groups and reactions are more qualitative than that of inorganic surfaces. [14], [28]. Also, by investigating the natural structures, it can be seen that biomolecules are structured by self-organization such as lipid bilayers, folding of nucleic acids etc. [13], [29], [30].

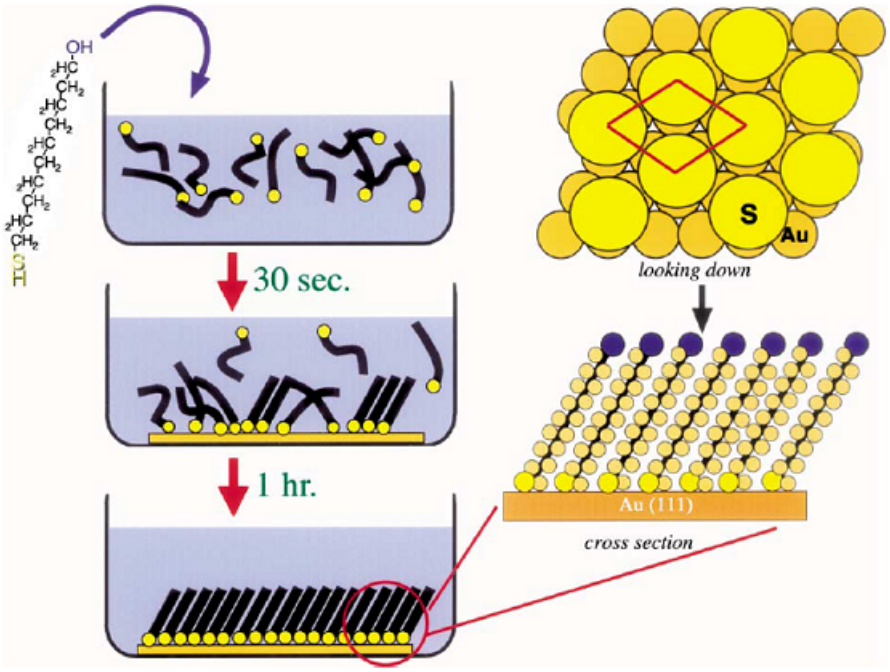

Figure 2.2 An example of Self Assembly Process (n-alkane modified gold surface) [14].

Self-assembled monolayers have a strong interaction with surface that can be covalently presented but it sometimes can bond to surface with non-covalent interaction while forming two-dimensional networks [27]. Traditional organic monolayer structure is performed by spreading insoluble compound to surface and after then by pressing it and most of these monolayers have formed by using Langmuir-Blodgett (LB) method. However, Whitesides et al. remarked that LB monolayers can be removed from surface by rinsing solvents. In order to prepare SAMs, the substrates are usually immersed in a solution at 25 °C with a time varying system [28], [31].

For the use of a well-designed surface, surface engineering applications have concentrated on biomolecule adsorption (especially proteins) and cell-surface interactions in biomaterial field. Chemical functionality, roughness, wettability, and surface charge properties of surfaces with SAMs are found as effective on cell and biomedical interactions [32].

According to specific reactions, by changing the terminal heads on the functional groups of SAMs with different molecules alterations have been observed [27]. A. Lan et al. and Curran et al. observed that cell proliferation and differentiation thereby phenotype and function of cells are related to surface chemistry [12], [33], [34]. The

functional groups such as amino-, carboxyl-, methyl, and hydroxyl- which are already present in natural structures affect the pre-protein layer characterization primarily. Later, integrins, which are transmembrane receptors on the cell wall, act as bridges between proteins and cell. These proteins on the surface bind to different regions of integrins so cell behaviors differ according to different proteins. These specific binding with their corresponding ligands on the cell wall is called *bio-recognition* process. In addition, immobilizing extracellular matrix proteins (ECM) such as laminin, fibronectin etc. and the molecules having similar assignment such as Poly-L-Ornithine and Poly-L-Lysine to surface can change the cell behavior because of the reasons explained above [12], [35].

Wettability represents intermolecular interactions at the solid-liquid surface by the aid of interfacial free energies. The quantitative analysis is made by contact angle measurement and the angle, θ, is taken as the tangent between drop and surface [31]. Nat et al. demonstrated that protein adsorption can increase with a decrease in the wettability of the surface. In addition, other studies indicated that hydrophobic proteins can be made accessible for interaction by denaturation since this process makes it easier to reveal the amino acids at the internal section so they can make a connection with the substrate surface. However, there is also another interaction between proteins which can make them enthalpically favorable like electrostatic interactions, Van der Waals interactions and hydrogen bonding. Although electrostatic interactions that arise from charged groups on amino acids and proteins are weaker than hydrophobic interactions, they can react with other opposite groups [12], [27], [32].

In some studies, different chemically modified surfaces have been investigated with different cell types and proteins. In Lin and Chuang study, human platelets have been investigated with -COOH, -CH_3, -OH and -SO_3H groups of SAMs and it has been found that the higher numbers of adherent platelets were observed on -COOH terminated SAMs and the lowest numbers were belong to -OH terminated SAMs [36]. In another study, Rodrigues et al. has been performed the adhesion of platelets under the influence of blood proteins and they found that an increase of -OH terminated alkanethiols caused a decrease in the fibrinogen adsorption [37]. In addition, human mononuclear and polymorphonuclear leukocytes have been investigated on -COOH, -OH and -CH_3 terminated SAMs and it was found that -CH_3 terminated had higher

number adherents but -OH terminated SAMs had also a higher number adherents [36]. Consequently, hydrophilic and hydrophobic surfaces are still not known in detail. Besides, they are not as good enough as moderate wettability for cell attachments. The moderate wettability makes possible adsorption of adequate proteins to surface by conserving its natural conformation [35].

2.3 The Effect of Histidine and Leucine Amino acids on Cell Behavior

Amino acids are defined as biologically important organic substances containing an amine (-NH_2) and carboxylic acid (-COOH) groups and along with a specific side chain in them. There are twenty-two essential that cannot be synthesized by organism and should be taken by diet.

Amino acids participate in metabolic pathways which are necessary for maintenance, growth, immunity and reproduction. They are structural units of peptides and proteins and also key precursors for hormones and nitrogenous substances. They are assigned for cell signaling, regulators of gene expression and protein phosphorylation cascade [38].

In this thesis, two amino acids, Histidine and Leucine, were used for experiments. Therefore, their functions in cell behavior will be discussed.

Histidine is a semi-essential amino acid that can be synthesized in very small amount in organism. However, this small amount of amino acids is made them essential for taking outside. Histidine is a basic, hydrophilic and polar amino acid with an aromatic nitrogen-heterocyclic imidazole side chain. Histidine takes part in a lot of reactions in metabolism such as protecting cells from damage caused by radiation, removing heavy metals from the body and repairing tissue. Also, it contributes to cell growth and proliferation, especially in fibroblast cells and it is essential for survival of cells [39], [40].

Leucine is an essential amino acid which has a branched chain and hydrophobic,

neutral and non-polar properties. Leucine is used in the sterol formation by organism. It takes part in the stimulation of muscle protein synthesis. Branched chain amino acids are great energy sources in skeletal muscle. Fibroblasts are believed to come from fibrocyte or smooth muscle cell linings. According to Graham et al., human skin fibroblasts, myoblasts, and fused muscle cells are grown in the presence of leucine [41]. Leucine is also essential for survival and it promotes growth activity [40]. Haff et al. stated that rabbit fibroblasts (strain RM3-56) require Leucine for proliferation of cells [39].

Based on previous studies, cells were found to be much more prone to hydrophilic surfaces in point of attachment [42]. Tamada and Ikada, 1993, observed that the optimal contact angle for cell adhesion is nearly 70° [42], [43]. Also, it was found that fibroblasts perform the highest cell adhesion between 60° and 80°. In addition, cells perform good proliferation, spreading and differentiation on hydrophilic surfaces [42]. Besides, the charge of surfaces has an effect on cell behavior. Studies show that positively charged surfaces induce the cell affinity and differentiation more than negatively charged surfaces [44]. The nature of amino acids is very complicated. The charges of the amino acids side chains can be varied through medium pH. Therefore, these differences can also influence the cell attachment, proliferation and differentiation.

3. MATERIALS AND METHODS

3.1 Surface Preparation

3.1.1 Cleaning of Si Wafer Substrates

Si wafers were used as a substrate to form mimicked micro-environment of L929 fibroblast cells. Si wafer was cut into 1x1 cm^2 pieces by using a diamond cutter. Cleaning process was done with an ultrasonic bath (Bandelin-Sonorex) in ethanol and distilled water, for 5 minutes each respectively. Then, substrates were dried with N_2 gas. After this process, the surfaces were activated with oxygen (O_2) plasma (March Plasma Systems, PM-100) for 10 min at 142 $\pm$ 2 mT and 50 sccm flow of oxygen to form -OH groups on the surfaces of Si wafers [45].

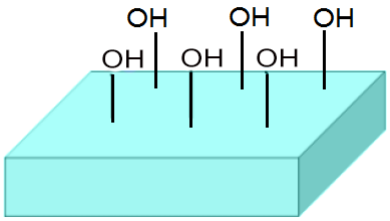

Figure 3.1 Activated Si Wafer Surface.

3.1.2 Chemical Modification of Si Wafer Substrates

After cleaning process, Si wafers were modified with amino acid conjugated self-assembled monolayers, (3-Aminopropyl)triethoxysilane (APTES) molecule and Poly-L-Ornithine.

3.1.2.1 Modification of Si Wafer Substrates with APTES.

42 mM APTES aqueous solution (v/v, in dI H_2O) was prepared and O_2 plasma treated substrates were immersed in the solution for 20 min at room temperature. After the reaction, substrates were washed with dI H_2O and dried with N_2 gas [45].

3.1.2.2 Modification of Si Wafer Substrates with Poly-L-Ornithine.

Cleaned substrates were coated with 15μg/mL Poly-L-Ornithine and waited in the incubator for 1h at 37°C. After this time, they were rinsed with PBS for 3-4 times. Then, they were waited under aspiration and put into 37°C incubator for drying procedure about 2h [46].

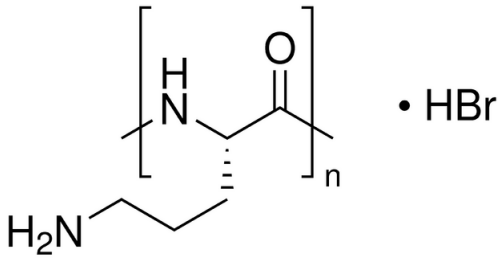

Figure 3.2 Chemical Structure of PLO.

3.1.2.3 Synthesis of Amino Acid Conjugated Self Assembled Molecules.

All chemicals were supplied from Sigma Aldrich, Merck. Dichloromethane (CH_2Cl_2) was purified with the presence of tetrahydrofuran (THF) benzophenone and used after boiling with sodium metal on calciumhydride (CaH_2). In an ice bath, solution of amino acid (1 equivalent) in NaOH (aq, 1,5 equivalent) was cooled. Cbz-Cl's (1,3 equivalent) solution in dioxane was added to the amino acid solution drop by drop. After this addition, the reaction mixture was mixed at 0°C for 30 min and at 25°C for 16h. Then, dioxane was evaporated under vacuum and extracted with ethyl acetate (3x25 mL). By

using 1M HCl, the pH of the liquid was fixed 2. Acidified liquid phase was extracted by using ethyl acetate (4x20mL). Organic phase was dried by using sodiumsulphate. The solvent was evaporated under vacuum so the amino acids; Cbz-His-Bt, and Cbz-Leu-Bt were synthesized [47] [48]. The characterization of His-SAM and Leu-SAM was done by using ^{1}H-NMR spectroscopy (Brueker, 500 MHz, Germany) in CDCl3, or DMSO-*d6*. Tetramethylsilane was used as an internal standard.

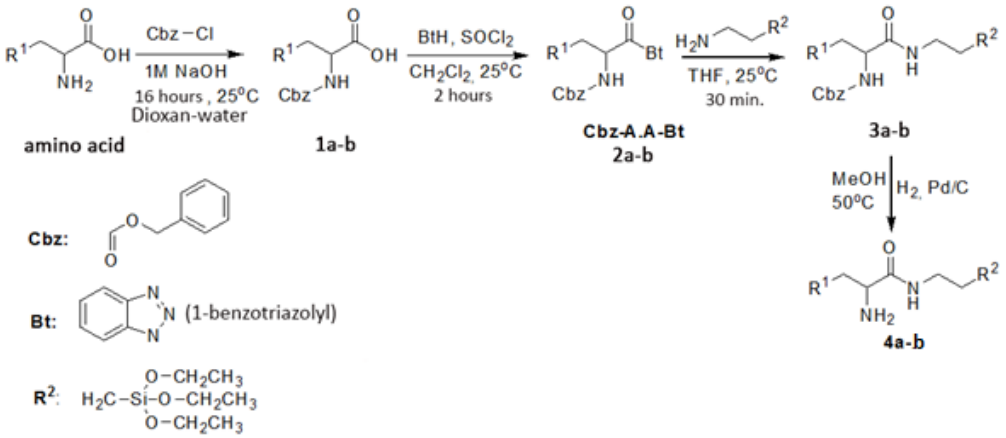

Figure 3.3 General Synthesis Procedure of Amino Acid Conjugated SAMs.

3.1.2.4 Modification of Si Wafer with Amino Acid Conjugated SAMs.

Amino acid conjugated self-assembled molecules (His-SAM and Leu-SAM) were prepared in the form of 20 mM solutions with ethanol. Cleaned Si wafers were modified with these amino acids to determine the formation of self-assembled monolayers on Si wafers with the effect of concentration (1-20 mM) and dipping times (30min-24h). Substrates were rinsed with ethanol and dried with N_2 gas after reactions were completed.

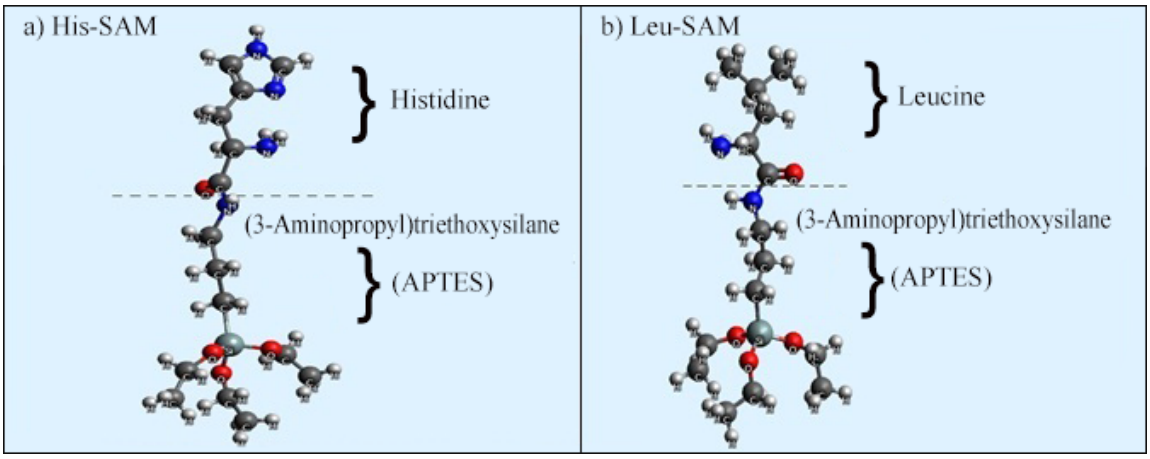

Figure 3.4 Histidine and Leucine Conjugated Self-Assembled Molecules.

3.2 Surface Characterization

3.2.1 Water Contact Angle Measurements

This method aims to investigate the wettability of substrate surfaces by the contact of solid-liquid interface. Bare, activated, APTES, PLO, His-SAM, and Leu-SAM modified Si wafer substrates were measured with the aid of Drop Shape Analyzer (DSA) 100, Krüss. Measurements were taken with fixed amount of distilled water drop (1 μL) at 25°C. For each modified, activated and bare substrates, measurements were taken from 5 regions of each sample. Static surface angles of the drop placed on the surface were measured within 1min. After measurements, data were obtained from the software and contact angles were calculated [49].

3.2.2 Atomic Force Microscopy (AFM)

By measuring the surface interaction forces, atomic force microscopy can obtain the surface topography of the sample. The surface roughness of bare, activated, APTES, PLO, His-SAM, and Leu-SAM and modified substrates were examined. By the way of processing data, the topographical images of the surfaces were obtained

with atomic resolution [49]. The measurements were performed at Hacettepe University Department of Chemistry.

3.2.3 X-Ray Photoelectron Spectroscopy (XPS)

The changes in the chemical composition of silicon wafer substrates were analyzed with X-Ray Photoelectron Spectroscopy (Thermo Scientific K-Alpha X-Ray Photoelecron Spectrometer) [50]. Measurement were taken by using Monochromated aluminum Kα radiation, at 72W, 400 μm spot size, 90° angle and with a 128-channel detector and performed at Boğaziçi University RD Center.

3.2.4 Ellipsometry

The thickness of the materials was measured by ellipsometry. The method is based on the change in the polarization of reflecting light from the material surfaces [50]. All thickness measurements were conducted with 65° angle of incidence and under 658 nm wavelength of green laser light. In the analysis of layer thickness, 50x50 μm regions were used for taking measurements. Si<100>/SiO2/Organic Layer/Air consisting phases were accepted as models. The measurements were performed at Hacettepe University Department of Chemistry with Auto-Nulling Ellipsometry, Nanofilm EP3. Also, theoretical thicknesses of molecules were measured by the aid of Avogadro Software (Hanwell, 2012, Open Source) [50].

3.2.5 UV-Visible Spectrophotometer

The quantitative analysis of Poly-L-Ornithine on the substrates was measured with Nanodrop 2000c Spectrophotometer (Thermo Scientific). The method is based on measuring the reflecting light from material as a function of its frequency or wavelength [51]. Calibration curve for PLO was given in Apendix A.

3.3 Cell Studies

Cell proliferation tests were carried out with L929 fibroblast cells. Cells with Dulbecco's modified Eagle's medium (DMEM) (with 10% Fetal Bovine Serum, 1% Penicilin/Streptomycin) were seeded into 24 well plates that include control, activated and modified samples. Cell density was adjusted as $1x10^5$ cells for per well. Samples were incubated at 37°C in a humidified atmosphere of 5% CO_2. The experiments proceeded at day 1 and 3.

3.3.1 Cell Proliferation

After 24h of incubation, DMEMs in each well were taken away and washed with PBS. PBS was shifted with 500 μL DMEM (with 2% Fetal Bovine Serum, 1% Penicilin/Streptomycin). Then, tetrazolium dye MTT 3-(4,5-dimethylthiazol-2-yl)-2,5-diphenyltetrazolium bromide (Sigma-Aldrich) that was dissolved in DMEM without phenol (5ml/mg) was added in the samples (75 μL for each) and waited for 3 hours to assess cell viability by the activity of enzymes reducing the dye. After 3 hours, the dye solutions were shifted with 500 acidified isopropanol solutions and 100 μL solutions for each well were transferred into 96 well plates in turn for spectrophotometric measurement (BIO-RAD iMark, Microplate Reader). The absorbance was measured at 570 and 750 nm, respectively. The same procedure was applied for the 3^{rd} day, again [52].

4. RESULTS

4.1 Characterization of Amino Acid Conjugated Self-Assembled Molecules

4.1.1 Nuclear Magnetic Resonance Spectroscopy (NMR) Analysis

His-SAM and Leu-SAM were synthesized as described in section 3.1.2.3. Leu-SAM and His-SAM were obtained as white microcrystals with 78% and 91% yield, respectively. His- SAM, white microcrystals were obtained with yield. After the reaction for His-SAM, non-isolated byproducts were obtained. This product's mixture was reacted with amines directly and Nuclear Magnetic Resonance (NMR) analysis was done from this mixture. Characterization of Cbz-Leu-Bt, Cbz-His-Bt, Leu-SAM and His-SAM was done by using NMR spectroscopy (Brueker, 500 MHz, Germany) in $CDCl_3$ or DMSO-*d6*. Tetramethylsilane was used as internal standard. NMR spectra of Cbz-Leu-Bt, Cbz-His-Bt, His-SAM, Leu-SAM and Trp-SAM were shown in Figure 4.1, 4.2, 4.3, 4.4.

For Cbz-Leu-Bt, ^{1}H-NMR (500 MHz, $CDCl_3$) δ: 8.30 (d, J= 8.23 Hz, 1H), 8.15 (d, J= 8.23 Hz, 1H), 7.69 (t, J= 7.25 Hz, 1H), 7.55 (t, J= 7.25 Hz, 1H), 7.42-7.34 (m, 5H), 5.87 (dt, J= 8.29, 4.88 Hz, 1H), 5.51 (d, J= 8.49 Hz, 1H), 3.70 (s, 2H), 2.00-170 (m, 3H), 1.15 (d, J = 5.34 Hz, 3H), 1.00 (d, J = 5.34 Hz, 3H) ppm.

For Cbz-His-Bt, ^{1}H NMR (500 MHz, DMSO-*d6*): δ = 9.13 (s, 1H), 8.54 (d, J = 7.2 Hz, 1H), 8.30 (q,J = 8.3 Hz, 2H), 7.82-7.87 (m, 1H),7.65-7.70 (m, 1H),7.54 (s, 1H), 7.30-7.37 (m, 5H),5.88 (q, J = 8.3 Hz, 1H), 5.06 (s, 2H), 3.46-3.50 (m, 1H), 3.35-3.43 (m, 1H).

For Leu-SAM, ^{1}H NMR (500 MHz, $CDCl_3$): δ = 6.24 (s, 1H), 5.30 (d, J= 8.18 Hz, 1H), 4.25 (wide, s, 2H), 4.15 (dt, J= 8.29, 4.88 Hz, 1H), 3.85 (q, J= 6.98 Hz, 6H), 3.28 (dt, J= 11.92, 6.35 Hz, 2H), 1.70-1.60 (m, 2H), 1.54 (p, J= 8.40 Hz, 2H), 1.24 (t, J= 6.98 Hz, 9H), 0.98-0.92 (m, 6H), 0.64 (t, J= 8.00 Hz, 2H) ppm.

For His-SAM, ^{1}H NMR (500 MHz, $CDCl_3$): δ = 10.2 (wide,s, 1H), 7.55 (s, 1H), 6.92 (s, 1H), 6.80 (s, 1H), 4.55-4.45 (m, 1H), 4.23 (wide, s, 2H), 3.85 (q, J= 6.90 Hz, 6H), 3.30-3.20 (m, 2H), 3.12 (wide, s, 1H), 2.98 (dd, J= 14,16, 5.00 Hz, 1H), 1.60-1.46 (m, 2H), 1.24 (t, J= 8.27 Hz, 9H), 0.50-0.40 (m, 2H) ppm. 13C NMR (125 MHz, CDCl3) δ = 7.5, 18.3, 22.7, 27.2, 29.7, 41.9, 45.0, 58.4, 119.5, 135.0, 136.2, 171.6ppm.

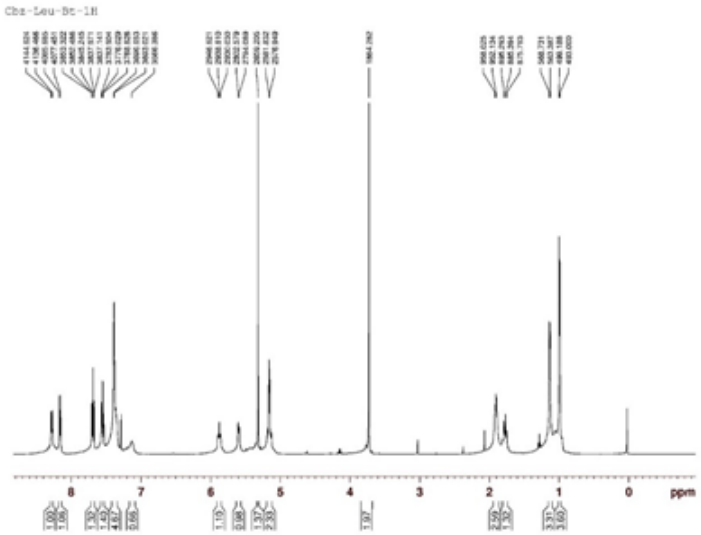

Figure 4.1 ^{1}H NMR spectrum of Cbz-Leu-Bt, Benzyl 1-(1H-benzo(d)(1,2,3)triazol-1-il)-4-methyl-1-oxopentane-2-ilcarbamade (2a).

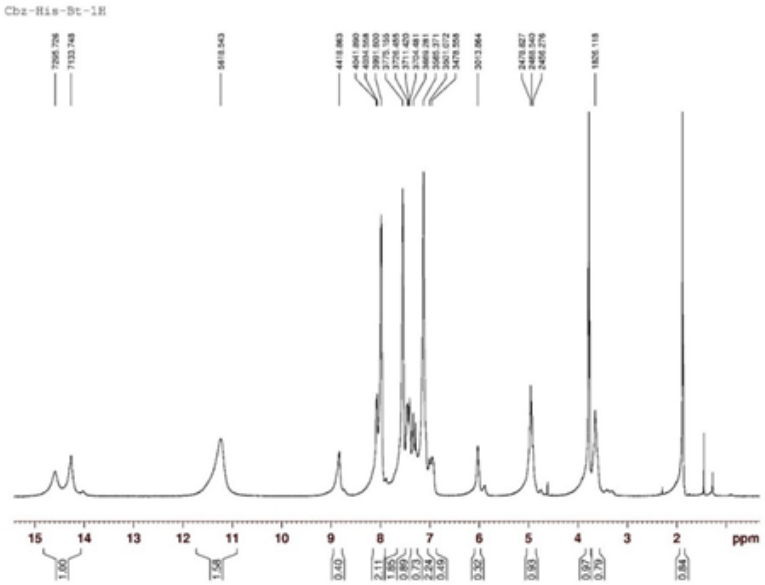

Figure 4.2 ^{1}H NMR spectrum of Cbz-His-Bt, Benzyl 1-(1H-benzo(d)(1,2,3)triazol-1-il)-3-(1H-imidazole-4-il)-1-oxopropane-2-ilcarbamade (2b).

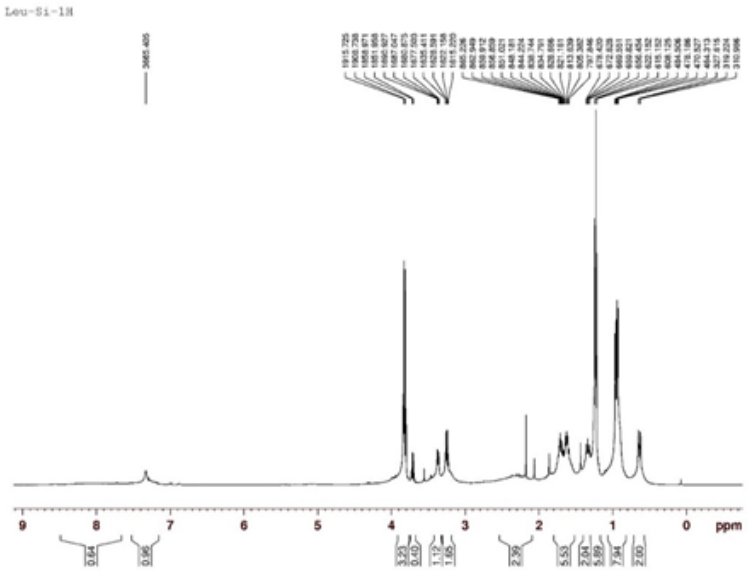

Figure 4.3 ^{1}H NMR spectrum of 2-Amino-4-methyl-N-(3-(triethoxysisily)propyl)pentane amide (4a).

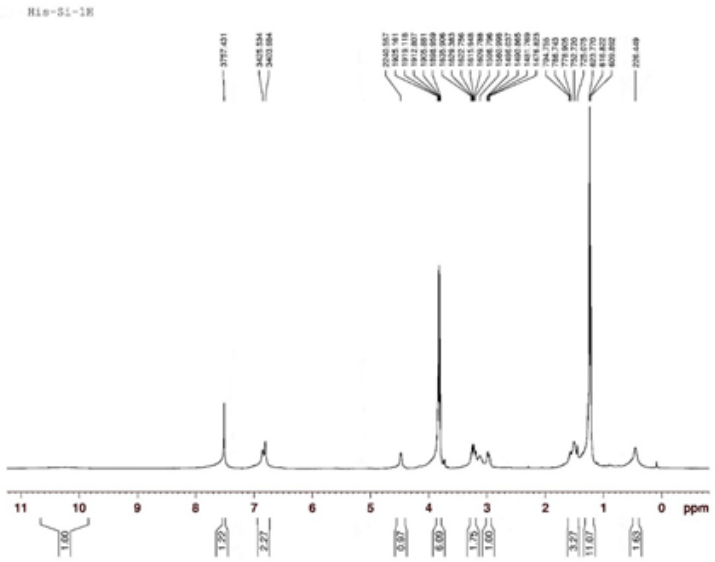

Figure 4.4 ^{1}H NMR spectrum of 2-Amino-3–(1H-imidazol-4-il)-N (3(triethoxysisily)propyl)pentane amide (4b).

4.1.2 Water Contact Angle and Ellipsometry Measurements

Contact angle and ellipsometry analysis of bare, activated, and 42 mM APTES (v/v, in dI H_2O) modified substrates were investigated. The results were shown in Table 4.1.

According to the results, 42 mM APTES modified Si wafers are more hydrophobic than bare and activated silicon wafers but it is approximately same hydrophobicity with His-SAM and more hydrophilic than Leu-SAM. After O_2 plasma, Si wafer surface was activated and formation of -OH groups on the surface of Si wafer resulted with more hydrophilic surfaces.

Table 4.1
Contact Angle and Ellipsometry Analysis of bare, activated and 42 mM APTES modified Si Wafer Substrates.

Samples	Contact Angle (°)
Si Wafer	36.2° ± 2.4
Activated Si Wafer	8.45° ± 1.10
42 mM APTES Modified Si Wafer	66.65° ± 3.12

Concentration experiments were done by using increasing concentrations of His-SAM (1-20 mM, w/v, in ethanol). The experiments were performed with a constant time (2h) at 25°C. Also, the thickness of the layers by His-SAM was investigated by ellipsometry. The results were shown in Table 4.2.

After modification with 1 mM and 2 mM His-SAM, the layer thickness was measured as 1.3 ± 0.3 nm and 1.2 ± 0.1 nm, respectively (Table 4.2). As a result of an increase in the molarity of His-SAM (5 mM and 10 mM), the layer thickness was decreased to 0.8 ± 0.2nm and 0.9 ± 0.1 nm, respectively. At the concentration of 20 mM, it was observed that there was an increase in the thickness of SAM. As the concentration of His-SAM increase from 2 mM to 10 mM, the contact angle results showed increasing hydrophobic values (68.3° ± 1.9 to 74.3° ± 1.4). At the concentration of 20 mM, it was observed that the hydrophobicity decreased (67.3° ± 0.6). According

Table 4.2
Contact Angle and Ellipsometry Results of His-SAM modified Si Wafer Substrates with the effect of different concentrations (1-20 mM); dipping time: 2h, in air, at 25°C.

Concentration (mM)	Contact Angle (°)	Thickness (nm)
1	48.8 ± 3.3	1.3 ± 0.3
2	68.3 ± 1.9	1.2 ± 0.1
5	71.6 ± 1.3	0.8 ± 0.2
10	74.3 ± 1.4	0.9 ± 0.1
20	67.3 ± 0.6	1.1 ± 0.1

to these results, the concentration was defined as 5 mM His-SAM for dipping studies.

After, cleaned Si wafer substrates were modified with increasing dipping times of 5 mM His-SAM (30 min-24 h, at 25°). Also, the thickness of the layers was measured by ellipsometry. The results were shown in Table 4.3.

Table 4.3
Contact Angle and Ellipsometry Results of His-SAM modified Si Wafer Substrates with the effect of different dipping times (30min-24h); in air, at 25°C.

Dipping Time	Contact Angle (°)	Thickness (nm)
30 min	62.1° ± 0.26	1.0 ± 0.1
1 h	59.5° ± 0.25	1.1 ± 0.1
2 h	71.6° ± 0.53	0.8 ± 0.2
4 h	72.1° ± 0.37	0.9 ± 0.1
24 h	73.6° ± 0.82	1.8 ± 0.1

The layer thickness of His-SAM was found as 1.0 ± 0.1 nm after 30 min. As a result of an increment in the dipping time, the thickness of His-SAM also showed an increase but the end of 4h, it was measured as 0.9 ± 0.1 nm. The layer thickness was found as 1.8 ± 0.1nm which is close to theoretical value (1.63 nm, Avogadro Software). After 30 minutes, the contact angle was measured as 62.1° ± 0.6. The hydrophobicity of His-SAM raised with the increase of dipping time except 1h. According to these results, the dipping time was defined as 1h for further studies.

Concentration experiments were performed with the same method by using increasing concentrations of Leu-SAM (1-20 mM, w/v, in ethanol). The experiments were performed with a constant time (2h) at 25°C. Also, the thickness of the layers by Leu-SAM was investigated by ellipsometry. The results were shown in Table 4.4.

Table 4.4
Contact Angle and Ellipsometry Results of Leu-SAM modified Si Wafer Substrates with the effect of different concentrations (1-20 mM); dipping time: 2h, in air, at 25°C.

Concentration (mM)	Contact Angle (°)	Thickness (nm)
1	74.2° ± 3.0	0.4 ± 0.1
2	88.1° ± 2.0	0.8 ± 0.1
5	104.4° ± 0.3	1.4 ± 0.3
10	108.3° ± 2.0	2.6 ± 0.2
20	124.1° ± 0.5	3.0 ± 0.1

According to Table 4.4, the film thickness increased from 0.4 ± 0.1nm to 3.0 ± 0.1 nm by the increase of concentration. Theoretical thickness of Leu-SAM was calculated as 1.57 nm with Avogadro Software. It was found that the thickness of 1 mM and 2 mM concentrations have low values from theoretical thickness. 5 mM concentration of Leu-SAM was showed a close relation with theoretical one.

After 5 mM, the thicknesses of layers exceeded the theoretical thickness. As a result of increment of the concentration, the hydrophobicity also increased from 74.2 ± 3.0 to 124.1° ± 0.5. According to these results, the concentration was defined as 5 mM for dipping time studies.

Subsequently, the dipping time experiments were performed for 5 mM Leu-SAM. The effects of increasing dipping times (30min-24h, at 25°C) on modified Si wafer substrates were investigated and the thickness of the layers by Leu-SAM was observed with ellipsometry. The results were shown in Table 4.5.

Table 4.5
Contact Angle and Ellipsometry Results of Leu-SAM modified Si Wafer Substrates with the effect of different dipping times (30min-24h); in air, at 25°C.

Dipping Time	Contact Angle (°)	Thickness (nm)
30 min	68.90 ± 0.82	1.1 ± 0.1
1 h	96.20 ± 1.63	1.2 ± 0.1
2 h	104.40 ± 0.12	1.4 ± 0.3
4 h	108.00 ± 0.20	1.5 ± 0.4
24 h	100.90 ± 0.29	1.4 ± 0.1

The layer thickness of Leu-SAM was found as 1.1 ± 0.1nm after 30 min. As a result of an increment in the dipping time, it was not observed a change in the layer thicknesses. Also, there was not an obvious change in hydrophobicity of the surface with the increment of dipping times. According to these results, the dipping time was defined as 2h.

Cleaned Si wafer substrates were coated with 15μg/mL Poly-L-Ornithine for one hour in an in incubator with 5% CO2, at 37°C. After the incubation PLO modified Si wafers were washed and rinsed with PBS. Contact angle of PLO was found to be 25.28° ± 0.88. It was investigated that Poly-L-Ornithine could provide a hydrophilic or hydrophobic surface depending on substrates [53], as shown a hydrophilic character because of activated Si wafer (8.45° ± 1.10) in this study.

4.1.3 Atomic Force Microscopy (AFM) Analysis

4.1.3.1 AFM Analysis of His-SAM and Leu-SAM Modified Si Wafers.

The surface roughness values were investigated with AFM. The effect of concentrations and dipping times over surface roughness was examined. For this purpose, activated and modified Si wafers with particular dipping times and concentrations were

chosen (Activated Si Wafer; 5 mM 2h and 24h; 20 mM 2h). The images were given in Figure 4.5 and Figure 4.6.

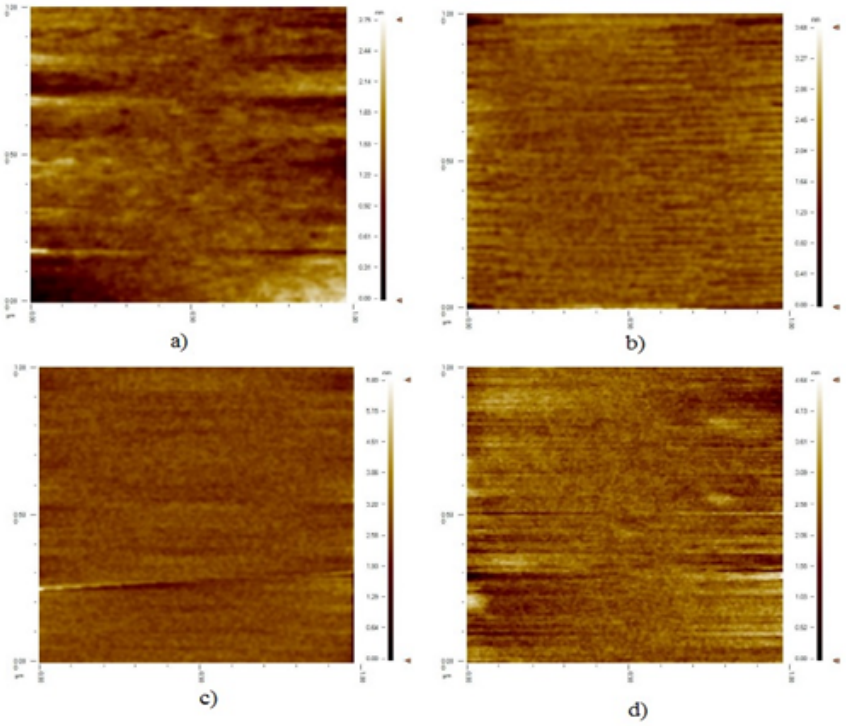

Figure 4.5 The images of activated and His-SAM modified Si wafer substrates a) Acitvated Si wafer b) 5 mM His-SAM modified Si wafer substrates for 2h c) 5 mM His-SAM modified Si wafer substrates for 24h d) 20 mM His-SAM modified Si wafer for 2h.

As seen from the images (Figure 4.5), surface modifications with His-SAM lead to changes in surface morphology. The roughness of bare Si wafer was measured as 0.21nm. The roughness values of 5 mM His-SAMs that were interacted with the surface for 2h and 24 were found as 0.15 nm and 0.33 nm. 20 mM His-SAM with 2h interaction time was measured as 0.18 nm. Here, it can be seen that dipping time has an effect on modification rather than concentration.

The surface modifications of Leu-SAM also lead to changes in surface morphology. The roughness of bare Si wafer was measured as 0.21 nm. The roughness values of 5 mM His-SAMs that were interacted with the surface for 2h and 24 were found as 0.20 nm and 0.31 nm. 20 mM His-SAM with 2h interaction time was measured as 0.17 nm. Again, it can be seen that dipping time has an effect on modification rather than concentration.

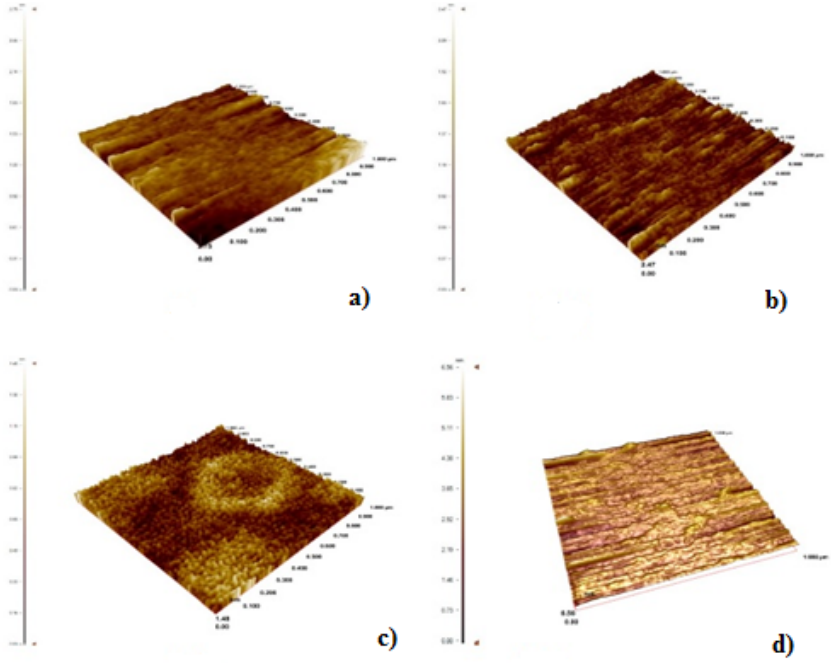

Figure 4.6 The images of activated and Leu-SAM modified Si wafer substrates a) Activated Si wafer b) 5 mM Leu-SAM modified Si wafer substrates for 2h c) 5 mM Leu-SAM modified Si wafer substrates for 24h d) 20 mM Leu-SAM modified Si wafer for 2h.

4.1.4 X-Ray Photoelectron Spectroscopy (XPS) Analysis

The bonds in the molecule structure of bare Si wafer and modified surfaces were analyzed with XPS. Characteristic signal areas of Si2p, C1s, N1s and O1s were investigated by obtaining spectra of activated, 42 mM APTES, His-SAM, and Leu-SAM modified Si wafers. Si2p, C1s, N1s, O1s signals were examined to correspond to 98.6 eV, 285.6 eV, 401 eV, 531.2 eV binding energies, respectively [54], [55]. Si2p signal can be observed as two peaks that are metallic Si and SiO_2.

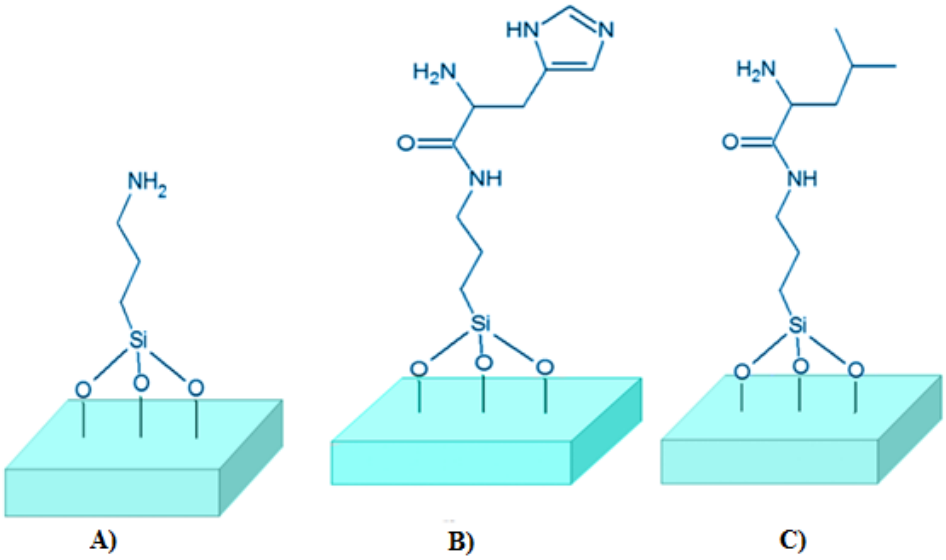

Figure 4.7 A) APTES, B) Histidine and C) Leucine modified Si wafers.

4.1.4.1 XPS Analysis of Activated Si Wafer.

The survey spectra of activated Si wafer were shown in Figure 4.8.

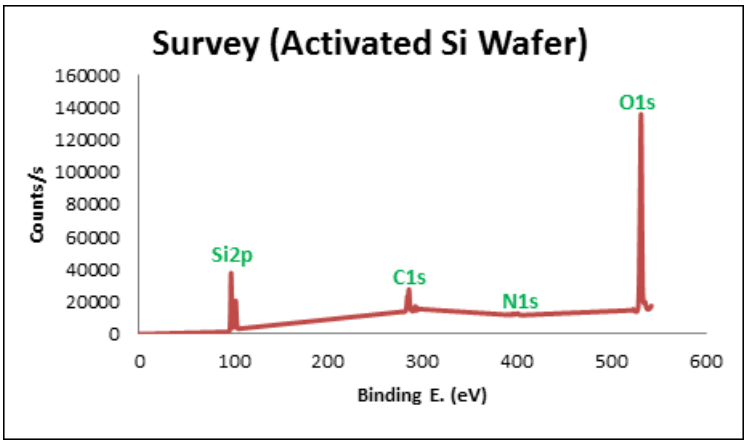

Figure 4.8 The survey spectra of activated Si wafer.

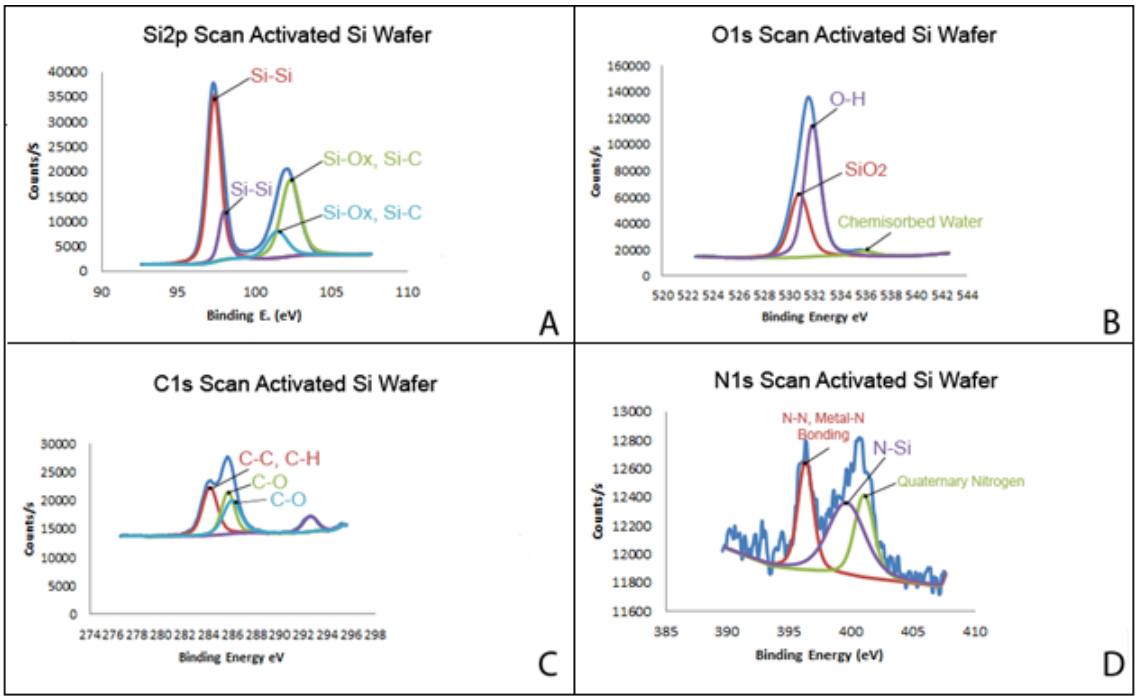

Figure 4.9 The XPS spectrum of Si2p, O1s, C1s, N1s regions of activated modified Si wafer and corresponding bonds.

According to each photoelectron spectrum (in Figure 4.8), bonds were examined through binding energies (eV). In the analysis of Si2p of activated Si wafer, Si-Si, Si-Ox/ Si-C peaks were found at 97.25 eV, 97.9 eV, 102.22 eV and 101.36 eV, respectively [56], [57]. In O1s photoelectron spectrum, SiO_2 and O-H bond was found at 530.7 eV and 531.73. Also, a peak was observed for chemisorbed water at 535.86 eV [58]. In C1s core level, C-C/C-H, C-O bonds corresponded to 284.01 eV, 285.53 eV and 285.86 eV, respectively [59]. Also, 396.2 eV, 400.93 eV and 399.39 eV corresponded to N-N/Metal-N bonding, quaternary nitrogen and N-Si. Normally, C and N atoms are not present in activated Si wafer. However, some bonds are available in the figure [60], [61]. It is thought that there may be a contamination in the sample.

4.1.4.2 XPS Analysis of APTES Modified Silicon Wafer.

The survey spectra of 42 mM APTES modified Si wafer were shown in the Figure 4.10.

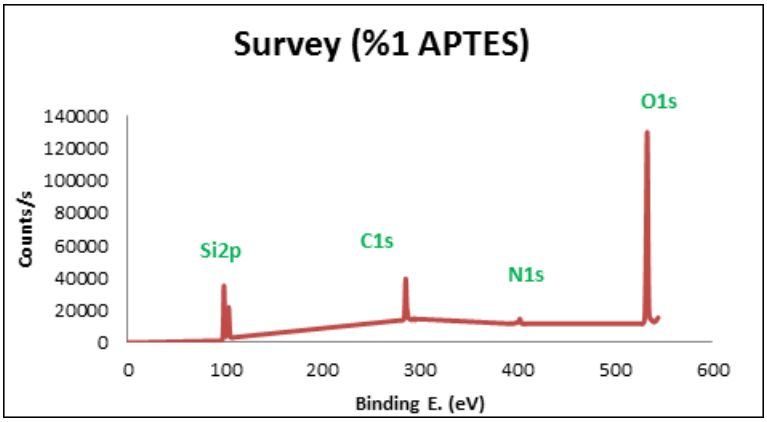

Figure 4.10 The survey spectra of APTES modified Si wafer.

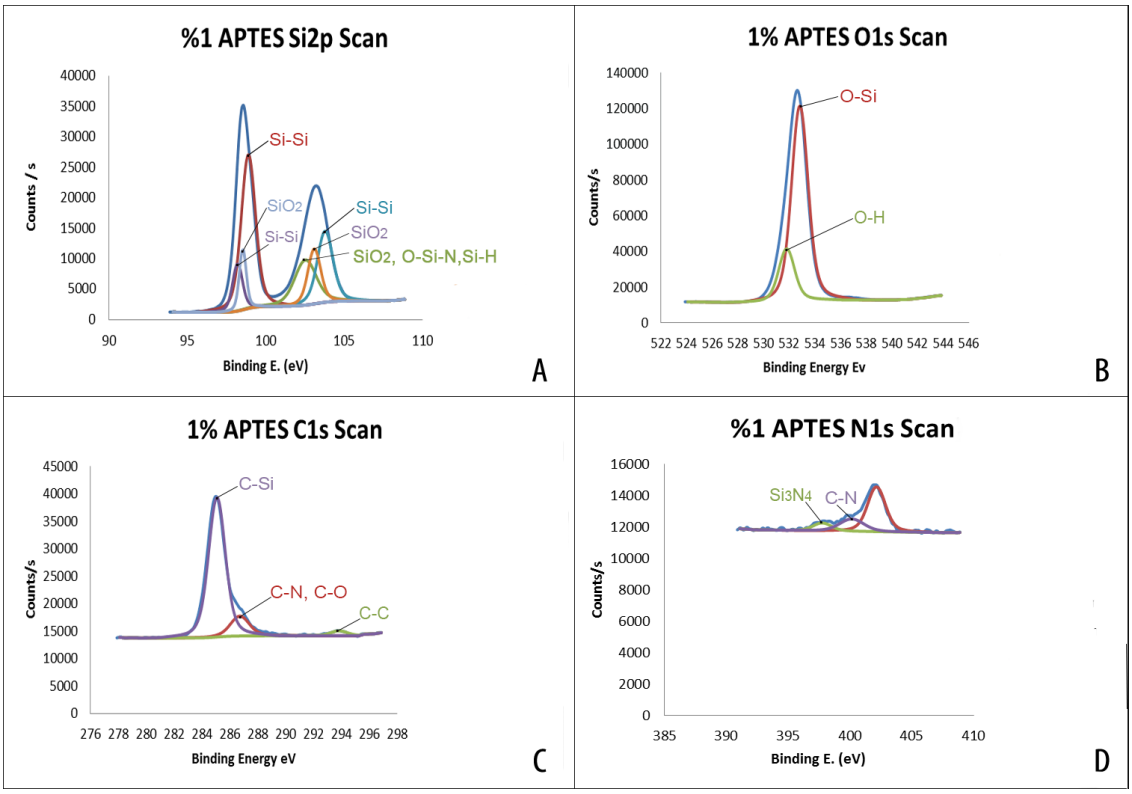

Figure 4.11 The XPS spectrum of Si2p, O1s, C1s, N1s regions of APTES modified Si wafer and corresponding bonds.

In Si2p core level, Si-Si bonds were observed around 98 eV. Si-O_2 bonds corresponded to 102.44 eV and 103.69 eV. O-Si-N/Si-H, Si-Ox bonds were found at 102.44 eV and 103 eV, respectively [62], [63], [64]. In O1s photoelectron spectrum, O-Si and O-H bond was found at 532.73 eV and 531.7 eV. In C1s core level, we can see the structure of the bonds of APTES molecules C-N/C-O, C-C, and C-Si bonds corresponding to 286.61 eV, 293.73 eV and 284.96 eV [65]. Also, 397.64 eV, 400.04 eV corresponded to Si_3N_4 and C-N.

4.1.4.3 XPS Analysis of His-SAM Modified Si Wafer.

The survey spectra of 5 mM His-SAM modified Si wafer were shown in the Figure 4.12.

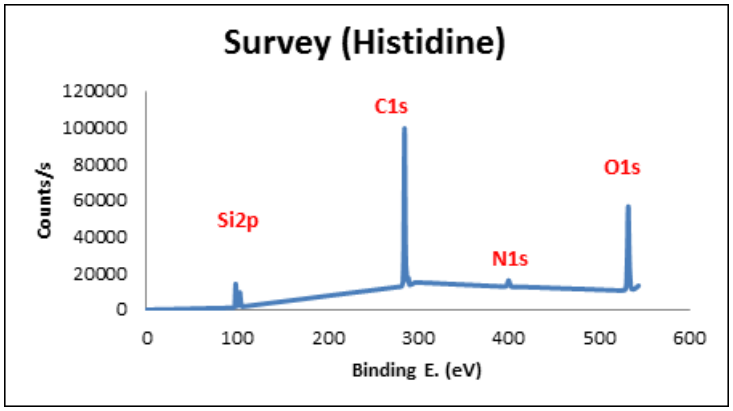

Figure 4.12 The survey spectra of His-SAM modified Si wafer

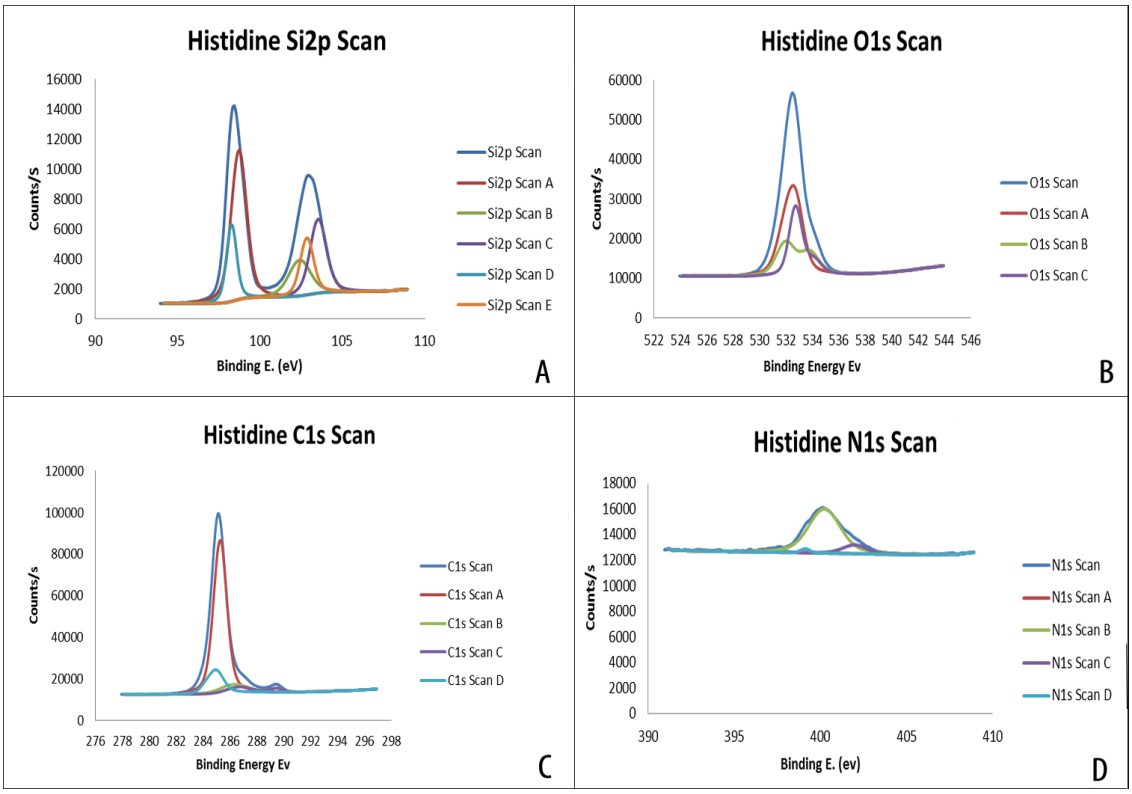

Figure 4.13 The XPS spectrum of Si2p, O1s, C1s, N1s regions of His-SAM modified Si wafer and corresponding bonds.

In Si2p spectrum, Si-Si bonds were observed at 98.61 eV, 98.16 eV, and 102.74 eV. Si-Ox bonds and Si-O bond were found at 102.27 eV, 103.42 eV and 102.74 eV, respectively [63]. Also, Si-C bonds were found at 102.27 eV and 102.74 eV [56], [57]. In O1s photoelectron spectrum, Si-O_2 corresponded to 533.21 eV. O-Si bonds were at 532.24 eV and 532.76 eV. In addition, C=O, C-N bonds which are in the imidazole ring of Histidine were observed at 289.46 eV and 286.69 eV. C-H/ C-O bonds, C-C/C-H bonds were found at 285.19 eV and 284.05 eV, respectively. N-H bonds also can be easily selected because of the imidazole ring of Histidine were at 401.89 eV. The other bonds that are Si_3N_4, N-C, and N-Si were seen at 397.15 eV, 400.13 eV and 399.04 eV, respectively [60], [61].

4.1.4.4 XPS Analysis of Leu-SAM Modified Si Wafer.

The survey spectra of 5 mM Leu-SAM modified Si wafer were shown in the Figure 4.14.

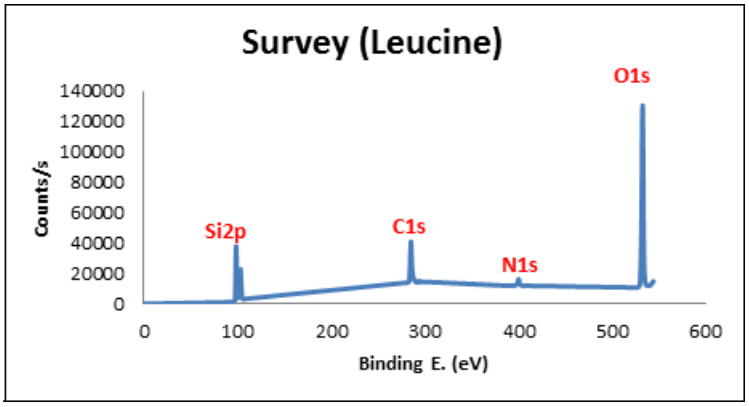

Figure 4.14 The survey spectra of Leu-SAM modified Si wafer.

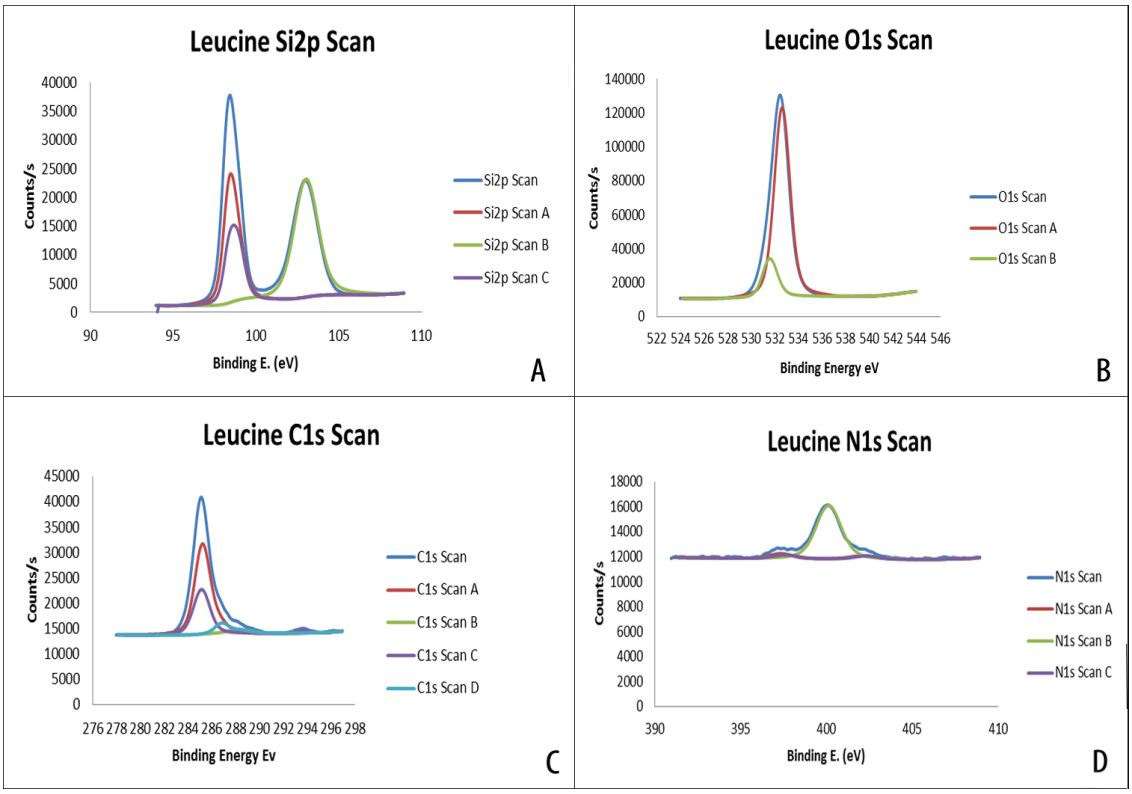

Figure 4.15 The XPS spectrum of Si2p, O1s, C1s, N1s regions of Leu-SAM modified Si wafer and corresponding bonds.

In Si2p core level, Si-Si bonds were observed at 98.46 eV, 98.49 eV and 102.93 eV. Si-O and Si-C bonds corresponded to 102.93 eV. In O1s photoelectron spectrum, O-Si and O-H bond was found at 532.49 eV and 531.45, respectively. In C1s core level, C-C was observed at 287.35 eV [65]. C-O bonds were seen at 285.75 eV, 286.62 eV, and 287.35 eV [65], [1]. C=O bond that exist in the Leucine structure was found at 286.62 eV. Also, C-N bond was found at the same binding energy.

4.1.5 Cell Studies

4.1.5.1 Cell Proliferation on Modified Si Wafers.

In order to understand proliferation effect, MTT test was applied on activated, PLO, APTES, His-SAM and Leu-SAM modified Si wafers with respect to control group (TCPS). Proliferation of L929 fibroblast cells on Si substrates at day 1 and 3

were determined using MTT assay (Figure 4.16). Activated Si wafer was chosen as a control, while PLO and APTS were chosen to compare our results with the conventional surface modifications [66], [67], [68], [69]. PLO was selected as a synthetic amino acid chain that is positively charged and generally used to plastic and glassware to increase cell attachment and adhesion. APTES was chosen to observe the effect of the amino groups on the proliferation of L929 fibroblast cells. At day one, all experimental groups have shown higher proliferation percentage than TCPS control group except His-SAM modified Si wafers (94.5 $\pm$ 6.9). The highest proliferation rate was measured on APTS modified Si wafers as 136.8 $\pm$ 9.6 with respect to control group (Figure 4.16 A)

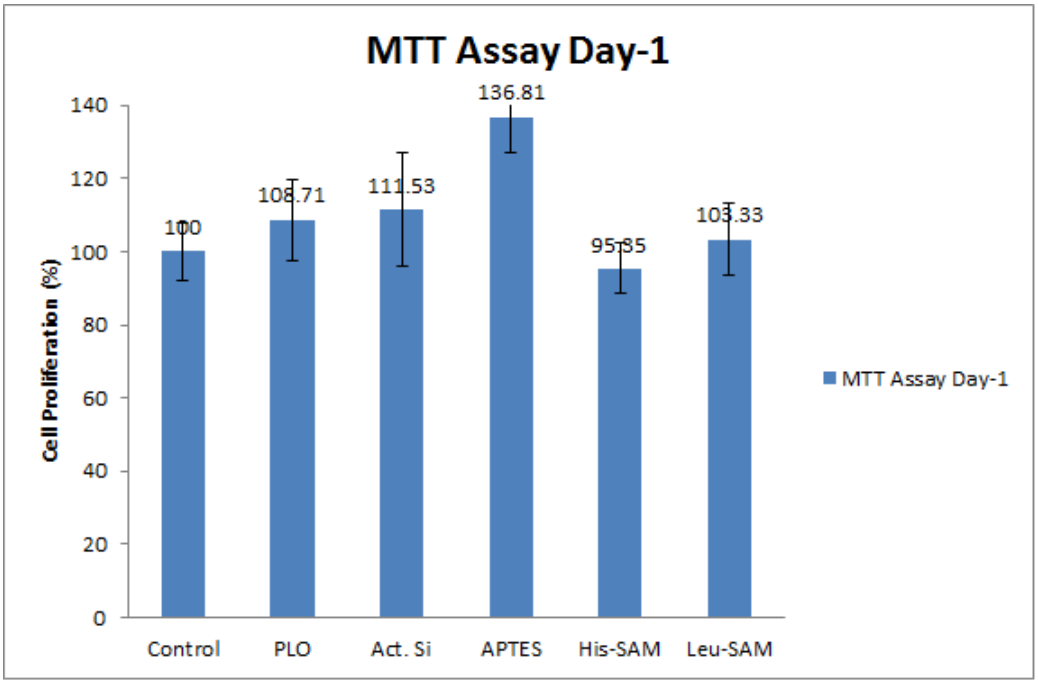

Figure 4.16 A) Results of the MTT assay: cell proliferation on the activated, PLO, APTES, His-SAM and Leu-SAM modified Si wafers after 24 h exposure.

At day three, all experimental groups have shown higher proliferation percentage than TCPS control group except His-SAM modified Si wafers (90.4 $\pm$ 6.9). The highest proliferation rate was measured on APTES modified Si wafers as 136.8 $\pm$ 2.4 with respect to control group like at day one. However, some of the experimental groupâs proliferation percentages were changed. When we compare, L929 Fibroblast cells proliferation it was increased from 108. 7 $\pm$ 11.1 to 120.4 $\pm$ 2.9 on PLO modified Si wafers. Activated Si, Leu-SAM and His-SAM modified Si wafers have shown similar

cell proliferation value like day one, as 109.9 ± 2.6, 103.8 ± 3.7, 90.4 ± 2.4, respectively. However, cell proliferation on APTES modified Si-wafers was decreased from 136.8 ± 9.6 to 105.1 ± 4.5.

According to 3^{rd} day of MTT results, all modifications have shown better or close proliferation when compared to control group (TCPS) (Figure 4.16 B). APTES modification have shown higher proliferation rate than Leu-SAM and His-SAM modification. However, APTES modification was not as stable as Leu-SAM and His-SAM modifications after three days. Activated Si also has shown a higher proliferation rate amino acid-SAM modified Si wafers and stable like amino acid-SAM modified Si wafers.

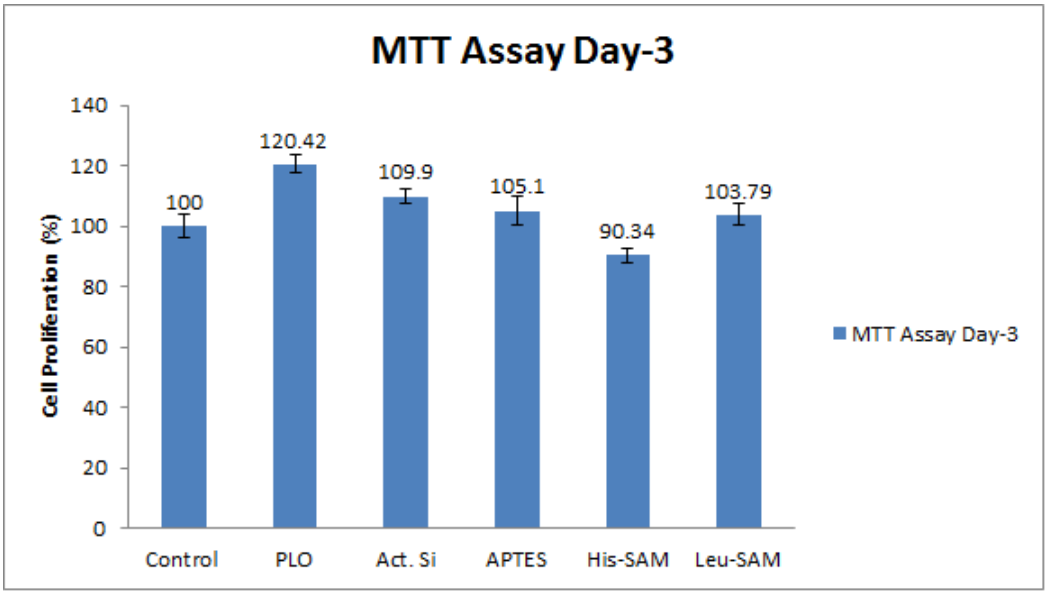

Figure 4.16 B) Results of the MTT assay: cell proliferation on the activated, PLO, APTES, His-SAM and Leu-SAM modified Si wafers after 72 h exposure.

5. DISCUSSION

5.1 Surface Modification and Analysis

In order to understand the importance of biological phenomena about biomaterials, cell like environments have been mimicked with different kind of molecules and with their modification on specific materials [6]. With the inspiration of these studies, fibroblast cells were tried to proliferate on newly synthesized-self assembled monolayers modified Si wafer surfaces. Before cell culture studies, characterization of modified Si substrates was carried out with different methods and techniques. Many parameters such as chemical groups on the surface, topography and hydrophobicity have an effect on cell behavior [70]. Thus, after characterization process, optimization of the parameters which has a substantial requirement for cell culture studies were performed.

Si wafer has been used for a decade in the medical applications but its effect on in vivo and in vitro studies has not still characterized well. However, it has not shown a cytotoxic effect on cell studies until now and it has been using a lot as medical devices such as semiconductors, biosensors, implants and microchips etc. [71]. Si wafer has a poor hemocompatibility compared with other materials using in the medical applications. However, its area of usage is increased by the modification techniques such as neural cell differentiation [72]. Thus, Si wafer is thought as a very promising material in biomedical field [71].

In this thesis, chemical modifications were done in order to optimize the surface of the material for obtaining an appropriate cell proliferation. However, substrate surface was cleaned and hydroxylated with O_2 plasma to carry out modification through -OH groups. Amino acid conjugated SAMs were tested in ethanol, acetone, tetrahydrofuran, toluene, CH_2Cl and CH_3Cl concentrations in order to investigate their solubility. His-SAM and Leu-SAM were soluble only in ethanol (Et-OH).

Modifications were performed with amino acid conjugated self-assembled molecules (His-SAM and Leu-SAM). In the characterization of these molecules, Cbz-AA-Bt was used as a protecting group for amines. At ^{1}H-NMR spectrum, doublet and triplet

signals that are belonged to benzotriazol molecule were observed at 8.15-8.30 ppm and 7.50-7.20 ppm, respectively. Also, the aromatic signal with 5 protons and the aliphatic signal with 2 protons that were observed at 7 ppm and 3.9 ppm, proves the presence of Cbz group in the reaction. After this step, the intermediate products (Cbz-AA-amines) were obtained through nucleophilic substitution of benzotriazol with amine groups and these products were determined with the signals at 3.0 ppm, 1.5 ppm and 0.6 ppm which are defined as the three methoxy group signals and the aliphatic -CH_2 signals of amines, respectively. At the end, the protecting groups were separated with catalytic hydrogenation method and the free amine functions were obtained.

APTES and PLO molecules were also used in the surface modification. APTES molecule has an amine group in the structure which gives the surface a hydrophilic property. Poly-L-Ornithine that act as extracellular matrix protein was used to provide cell growth, differentiation and proliferation.

For investigating the success of modifications, the results obtained from contact angle, ellipsometry, AFM and XPS techniques were analyzed. The contanct angle of Si wafer were measured as 36.2° ± 2.4. After plasma treatment, contact angle was measured as 8.45° ± 1.10 because of the hydroxylated surface of the Si wafer. The contanct angle of 42 mM APTES modified Si wafer was found as 66.56° ± 3.12. As this value is smaller than 90°, it can be accepted as semi-hydrophilic because of the amine groups of the APTES molecule.

In ellipsometry analysis of His-SAM modification, ellipsometry values for 1 mM, 2 mM, 5 mM, 10 mM and 20 mM correspond to 1.3 ± 0.3 nm, 1.2 ± 0.1 nm, 0.8 ± 0.2, 0.9 ± 0.1 nm, and 1.1 ± 0.1 nm, respectively. Theoretical thickness of the His-SAM was measured as 1.63 nm using the Avagadro Software (Hanwell, 2012, open source). This value is valid when the angle between His-SAM and the surface is equal to 90° .Thickness value obtained by measurements found to be lower than mentioned theoretical value, this circumstance would be attributed to interaction of the His-SAM with the surface at a certain angle. Surface shows hydrophilic characteristic at the concentration of 1 mM His-SAM (48.8° ± 3.3). Such high hydrophilic surface characteristic would be due to non-bonding presence of both the imidazole involved in Histidine and carboxylic acid groups or almost complete coating of the surface by His-SAM. Hence, at this concentration a thinner layer is acquired. This outcome indicates that His-SAM

interacts with the surface in a more perpendicular angle. As the His-SAM concentration increases from 2 mM to 10 mM, contact angle value passes to hydrophobic range (from 68.3° ± 1.9 to 74.3° ± 1.4). Within this range His-SAM orients with a certain angle and cause polar groups (imidazole and carboxylic acid) to repulse each others or mask. As a result of this, hydrophobic alkyl groups within the structure of the 3-aminopropyltriethoxysilane (APTES) come into view and hydrophobic effect was increased. Contact angle value was decreased when the His-SAM concentration is 20 mM (67.3° ± 0.6). This decrease in the contact angle value would be clarified by volumetric shift depending upon the additional rise in the concentration of His-SAM. Imidazole groups located on the side chain of the Histidine amino acid are pushed towards the outer surface of the SAM formed due to steric restriction that lead an attempt to make room for His-SAM and interact with a more perpendicular degree. Consequently, hydrophilic groups would be come to the view again due to an increment in the coating area of the His-SAM and the shift of the imidazole groups towards out.

In dipping time measurements, the layer thickness of His-SAM was found as 1.0 ± 0.1nm after 30 min. As a result of an increment in the dipping time, the thickness of His-SAM also showed an increase but the end of 4h, it was measured as 0.9 ± 0.1 nm. The layer thickness was found as 1.8 ± 0.1nm which is close to theoretical value (1.63 nm). After 30 minute, the contact angle was measured as 62.1° ± 0.6. Since it is previously known that measured thickness value is 1.0 ± 0.1nm in 30 minutes of dipping time an interpretation would be made that His-SAM is oriented by making a certain angle with the surface. Surface hydrophobicity increases with the increasing dipping time. As it was discussed in the effect of the concentration, quantifying the thickness of the His-SAM thickness as 0.9 ± 1.0 nm at the end of the 4 hours would be proceeded from the emergence of the hydrophobic alkyl groups which were originated from the structure of the 3-aminopropyltriethoxysilane (APTES) resulted by the orientation of the His-SAM with the surface at a certain angle. At the end of the 24 hours, thickness of the His-SAM was measured as 1.8 ± 0.1 nm. Although this value is close to the theoratical thickness value of the His-SAM, it is not possible for the molecule to interact perpendicularly with the surface, since there was no alteration in the hydrophobicity. This increment would be clarified by the reorientation of the surface molecules for the closely coated morphology and the overall coating or the formation of the duple or

multiple layers of the His-SAM molecules on the surface instead of a single layer in some sections where orientation is not observed. However surface roughness was not affected by the concentration, dipping time had an effect on it. As this alteration was discussed in the immersion effect, reorientation of the molecules which were connected to the surface for the closely coated morphology and the overall coating or formation of the doublet or multiple layers of the His-SAM molecules on the surface instead of a single layer in some sections where orientation was not observed. At the end, the concentration and dipping time for His-SAM was defined as 5 mM and 1h.

In Leu-SAM experiments, it was found that when the concentration is 1 mM or 2 mM, formed layer thickness was lower than the theoretical value. This observation would be attributed to the interaction of the Leu-SAM with the surface with a certain angle or incomplete coating of the surface. At the concentration of the 5 mM, measured thickness of the Leu-SAM is found so close to the theoretical value. It would be asserted that Leu-SAM forms a single layered structure at this concentration. Depending on the increment of the concentration to 10 mM and 20 mM, measured film thickness values were higher than the theoretical value. This result would be identified with the reorientation of the molecules which were connected to the surface for the closely coated morphology and the overall coating or formation of the doublet or multiple layers of the Leu-SAM molecules on the surface instead of a single layer in some sections where orientation was not observed. Hydrophobicity of the surface increased to the $124.1^\circ \pm 0.5$ from $74.2^\circ \pm 3.0$ as the concentration of the Leu-SAM was increased (1-20 mM). When the contact angle and the thickness values which were obtained at 1 and 2 mM Leu-SAM concentration were compared, it was inspected that Leu-SAMs are interacted with the surface in different angles.This conclusion would be attributed to the predisposition of the methyl groups located at the side chain of the leucine that provides hydrophobic characteristic to the molecule to interact within themselves rather than with the surface. This case directs corboxylic acid and so forth groups which were found in Leu-SAM to the surface and results in low hydrophobicity. At the concentration of 5 mM Leu-SAM the surface has shown hydrophobic characteristic. In addition, measured layer thickness (1.4 ± 0.3 nm) is found close to the theoratical value. For this case it would be projected that methyl groups located at the side chain of the leucine are within reach. At higher Leu-SAM concentrations like

10 and 20 mM, both of the hydrophobicity and layer thickness increased. Increase in the thickness would cause the reorientation of the surface molecules for the closely coated morphology and the overall coating or the formation of the duple or multiple layers of the Leu-SAM molecules on the where orientation is not observed. In addition, emergence of the hydrophobic alkyl groups originated from the structure of the 3-aminopropyltriethoxysilane (APTES) would lead to an increment in the number of the hydrophobic groups and in the contact angle value on this layers.

In dipping time experiment of Leu-SAM, the layer thickness was found as 1.1 $\pm$ 0.1nm after 30 min. Since it is known beforehand that the measured thickness value is equal to 1.1 nm for 30 minutes of immersion time, the conclusion can be drawn that Leu-SAM orientates with the surface in a certain angle. Increased dipping time does not lead to a sizable change in the surface hydrophobicity and thickness. It also can be asserted that Leu-SAM forms a stable layer. However surface roughness is not affected by the concentration, dipping time time has an effect on it. This alternation can be arisen from the reorientation of the molecules bonded to the surface within the signified time. In the end, the concentration and dipping time for Leu-SAM was defined as 5 mM and 2h.

The bonds in the molecule structure of bare and modified Si wafer surfaces were analyzed with XPS. Characteristic signal areas of Si2p, C1s, N1s and O1s were investigated by obtaining spectra of activated, 42 mM APTES, His-SAM, and Leu-SAM modified Si wafers. Si2p, C1s, N1s, O1s signals were examined to correspond to 98.6 eV, 285.6 eV, 401 eV, 531.2 eV binding energies, respectively [54], [55]. Si2p signal can be observed as two peaks that are metallic Si and SiO_2. As against the unmodified Si surface, a decrement was observed in the magnitude of the corresponding peaks of the metallic and SiO_2 on the surfaces coated with His-SAM. This data implies that His-SAM coats the surface more when it is compared to Leu-SAM and APTES. O1s signal is occurred at the lowest value for the His-SAM, this situation can be related to the comparison of the coating rates as aforesaid. When the N1s signal is investigated, there was no peak observed for activated Si wafer owing to the absence of the N atom in its structure. In addition to this, peak magnitude of the APTES molecule which involves 1 N atom is found to be lower both of than Leu-SAM that involves 2 N atoms and His-SAM that involves 4 N atoms. Peak with the highest magnitude is observed

for the His-SAM, when C1s peak is investigated. This peak indicates surface SAM accumulation clearly in itself.

5.2 Cell Studies

Proliferation of L929 cells on the on activated, PLO, APTES, His-SAM and Leu-SAM modified Si wafers with respect to control group (TCPS) at days 1 and 3 were determined using MTT assay [66]. His-SAM and Leu-SAM modification on cellular behavior were investigated according to the proliferation percent versus control groups. The number of cells on APTES modified Si wafers has shown the highest proliferation rate among all other experimental groups as 136.8 ± 9.6 at day one [73], [74]. Interestingly, O_2 plasma activated Si wafers also have shown high proliferation percentages (111.5 ± 15.4) [75], [76]. According to the contact angle measurements, bare, activated, APTES and PLO modified Si wafers were found to be, 36.2° ± 2.4, 8.45° ± 1.10, 66.56° ± 3.12, 25.28° ± 0.88, respectively. The contact angle of TCPS has been specified as 35 ° [77]. Activation was done by O_2 plasma and main purpose for doing this procedure to clean the surface and create -OH groups on Si wafer. After incubation of Si wafer in cell studies -OH groups will disappear and SiO_2 layer will form again which increases the contact angle value (from 8.45° ± 1.10 to 36.2° ± 2.4). We can say that the activated Si wafers contact angle will be similar after sometime like bare Si wafers. His-SAM modified Si wafer contact angle was found to be 59.5° ± 0.25 and while Leu-SAM was 104.4° ± 0.3. From the first day proliferation data, we can conclude that, L929 fibroblast cells do like more hydrophilic surfaces than hydrophobic surfaces [78], [79]. Histidine is an amino acid has a hydropaty index of -3.2 which means a hydrophilic molecule [80]. Histidine is a basic and essential amino acid with a positively charged imidazole ring which also gave a biofunctional property to the modified surfaces. Since the contact angle value of APTES modified surface is very close to His-SAM modified Si wafers, including the surface wettability, surface chemistry play a vital role in cellular behavior [44], [81]. Amino (-NH2) groups of APTES molecules have shown better cell proliferation than His-SAM molecules at day

one. Also, small NH_2 groups of APTES in may increase the accessibility of these groups during the interaction with L929 cells. Compared to APTES amino groups, His and Leu amino acids have large side chains such as imidazole ring and aliphatic isobuthyl that may be resulted with a steric hindrance when interaction with receptors of fibroblast cells [82].

At day 3, the highest proliferation percentage was observed on PLO modified Si wafers. There is a slight increase in the proliferation percentage of PLO modified Si wafers while there is a sharp decrease on the proliferation percentage of APTES modified Si wafers from 136.8 ± 9.6 to 105.1 ± 4.6. While there were no significant changes on the proliferation percentage of activated, Leu- modified and His-SAM Si wafers as 109.9 ± 2.6 , 103.8 ± 3.7 and 90.4 ± 2.5, respectively. At day one, it was clear that amino groups has a positive effect on the proliferation. In the ornithine's molecular structure there is one more amino group and because of this extra amino group, the structure may become more stable and/or increase the interactions with L929 fibroblast cells. Cui et al., investigated the effect PLO on proliferation of insulin-producing β cells from rat insulinoma (Rin-m5F cells) entrapped in alginate microcapsules, and observed an effect of PLO modification as an increase in the proliferation [83]. The decrease of proliferation on APTES modified Si wafer may be due to instability of APTES molecule on the surface. On the other side, His-SAM and Leu-SAM modified Si wafers have shown lower proliferation than the other experimental groups. However, after 3 days they have shown more stable proliferation percentages. Of course, only proliferation data does not give all the information about cellular behavior to these surfaces. Adhesion, morphology and viability studies must be performed for understanding the whole picture. By culturing different type of cell, we assume much more different cellular behavior on His-SAM and Leu-SAM modified surfaces.

5.3 Future Studies

The characterization of Si wafer substrates was supported with this study. For the next step, the adhesion, viability and morphology characterization of L929 cells will be continued. Also, new type cells will be studied to understand the underlying responses of biological behavior to these surface.

APPENDIX A. CALIBRATION CURVE OF PLO

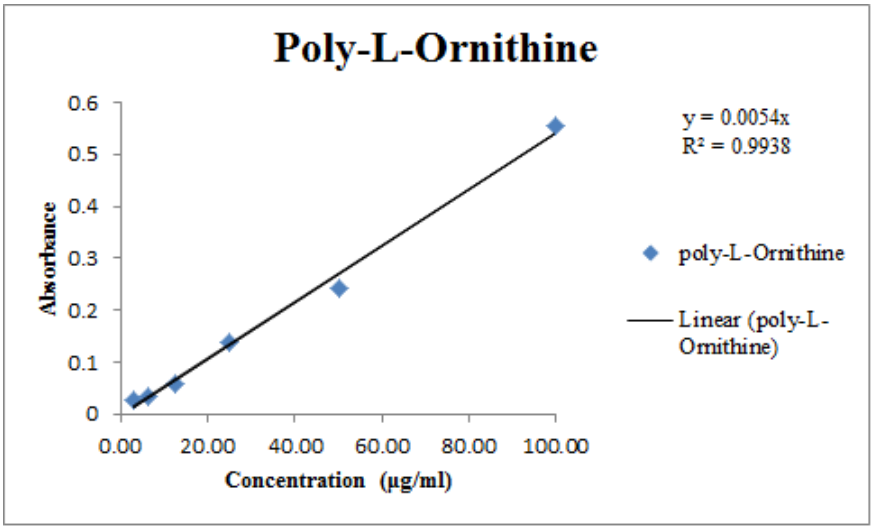

Figure A.1 Poly-L-Ornithine Calibration Curve at 203 nm.

REFERENCES

1. Huebsch, N., and D. J. Mooney, "Inspiration and application in the evolution of biomaterials.," *Nature*, Vol. 462, pp. 426–432, Nov 2009.

2. Zhang, S., "Emerging biological materials through molecular self-assembly.," *Biotechnol Adv*, Vol. 20, pp. 321–339, Dec 2002.

3. Ma, P. X., "Biomimetic materials for tissue engineering.," *Adv Drug Deliv Rev*, Vol. 60, pp. 184–198, Jan 2008.

4. Stevens, M. M., and J. H. George, "Exploring and engineering the cell surface interface.," *Science*, Vol. 310, pp. 1135–1138, Nov 2005.

5. Whitesides, G. M., and B. Grzybowski, "Self-assembly at all scales," *Science*, Vol. 295, pp. 2418–2421, Mar 2002.

6. Zhang, S., L. Yan, M. Altman, M. Lssle, H. Nugent, F. Frankel, D. A. Lauffenburger, G. M. Whitesides, and A. Rich, "Biological surface engineering: a simple system for cell pattern formation.," *Biomaterials*, Vol. 20, pp. 1213–1220, Jul 1999.

7. Newton, L., T. Slater, N. Clarka, and A. Vijayaraghavan, "Self assembled monolayers (sams) on metallic surfaces (gold and graphene) for electronic applications," *J. Mater. Chem. C*, Vol. 1, pp. 376–393, 2003.

8. Faucheux, N., R. Schweiss, K. Ltzow, C. Werner, and T. Groth, "Self-assembled monolayers with different terminating groups as model substrates for cell adhesion studies.," *Biomaterials*, Vol. 25, pp. 2721–2730, Jun 2004.

9. Ostuni, E., L. Yan, and G. M. Whitesides, "The interaction of proteins and cells with self-assembled monolayers of alkanethiolates on gold and silver," *Colloids and surfaces B: Biointerfaces*, Vol. 15, pp. 3–30, 1999.

10. Ratner, B. D., *Biomaterials science: an introduction to materials in medicine*, Academic Press, 2004.

11. Ratner, B. D., "New ideas in biomaterials science–a path to engineered biomaterials.," *J Biomed Mater Res*, Vol. 27, pp. 837–850, Jul 1993.

12. Roach, P., D. Eglin, K. Rohde, and C. C. Perry, "Modern biomaterials: a review - bulk properties and implications of surface modifications.," *J Mater Sci Mater Med*, Vol. 18, pp. 1263–1277, Jul 2007.

13. Tirrell, M., E. Kokkoli, and M. Biesalski, "The role of surface science in bioengineered materials," *Surf. Sci.*, Vol. 500 (1-3), pp. 61–83, 2002.

14. Castner, D. G., and B. D. Ratner, "Biomedical surface science: foundations to frontiers," *Surf. Sci.*, Vol. 500 (1-3), pp. 28–60, 2002.

15. Duke, C. B., "The birth and evolution of surface science: child of the union of science and technology.," *Proc Natl Acad Sci U S A*, Vol. 100, pp. 3858–3864, Apr 2003.

16. Kurella, A., and N. B. Dahotre, "Review paper: surface modification for bioimplants: the role of laser surface engineering.," *J Biomater Appl*, Vol. 20, pp. 5–50, Jul 2005.

17. Kasemo, B., "Biological surface science," *Current Opinion in Solid State and Materials Science*, Vol. 3, no. 5, pp. 451 – 459, 1998.

18. Thiel, P. A., and T. E. Madey, "The interaction of water with solid surfaces: Fundamental aspects," *Surface Science Reports*, Vol. 7, no. 6â8, pp. 211 – 385, 1987.

19. Henderson, M. A., "The interaction of water with solid surfaces: fundamental aspects revisited," *Surface Science Reports*, Vol. 46, no. 1â8, pp. 1 – 308, 2002.

20. Kasemo, B., "Biological surface science," *Surface Science*, Vol. 500, no. 1â3, pp. 656 – 677, 2002.

21. Gissler, W., and H. Jehn, *Advanced techniques for surface engineering*, Springer, 1992.

22. Kennedy, D., Y. Xue, and M. Mihaylova, "Current and future applications of surface engineering," *The Engineers Journal*, Vol. 59, pp. 287–292, 2005.

23. Poncin-Epaillard, F., and G. Legeay, "Surface engineering of biomaterials with plasma techniques.," *J Biomater Sci Polym Ed*, Vol. 14, no. 10, pp. 1005–1028, 2003.

24. Conrad, J. R., J. L. Radtke, R. A. Dodd, F. J. Worzala, and N. C. Tran, "Plasma source ion implantation technique for surface modification of materials," *Journal of Applied Physics*, Vol. 62, no. 11, pp. 4591–4596, 1987.

25. Ulman, A., "Formation and structure of self-assembled monolayers," *Chem. Rev.*, Vol. 96, pp. 1533–1554, 1996.

26. DiBenedetto, S. A., A. Facchetti, M. A. Ratner, and T. J. Marks, "Molecular self-assembled monolayers and multilayers for organic and unconventional inorganic thin-film transistor applications," *Advanced Materials*, Vol. 21, no. 14-15, pp. 1407–1433, 2009.

27. Nath, N., J. Hyun, H. Ma, and A. Chilkoti, "Surface engineering strategies for control of protein and cell interactions," *Surface Science*, Vol. 570, no. 1â2, pp. 98 – 110, 2004. {BIOSURF} V: Functional Polymeric Surfaces in Biotechnology.

28. Whitesides, G. M., and P. E. Laibinis, "Wet chemical approaches to the characterization of organic surfaces: self-assembled monolayers, wetting, and the physical-organic chemistry of the solid-liquid interface," *Langmuir*, Vol. 6, no. 1, pp. 87–96, 1990.

29. Zhang, S., "Fabrication of novel biomaterials through molecular self-assembly.," *Nat Biotechnol*, Vol. 21, pp. 1171–1178, Oct 2003.

30. Whitesides, G. M., and M. Boncheva, "Beyond molecules: self-assembly of mesoscopic and macroscopic components.," *Proc Natl Acad Sci U S A*, Vol. 99, pp. 4769–4774, Apr 2002.

31. Bain, C. D., and G. M. Whitesides, "Modeling organic surfaces with self-assembled aonolayers," *Angew. Chem. Int. Ed. Engl.*, Vol. 28, no. 4, pp. 506–512, 1989.

32. Arima, Y., and H. Iwata, "Effect of wettability and surface functional groups on protein adsorption and cell adhesion using well-defined mixed self-assembled monolayers.," *Biomaterials*, Vol. 28, pp. 3074–3082, Jul 2007.

33. Curran, J. M., R. Chen, and J. A. Hunt, "Controlling the phenotype and function of mesenchymal stem cells in vitro by adhesion to silane-modified clean glass surfaces.," *Biomaterials*, Vol. 26, pp. 7057–7067, Dec 2005.

34. Lan, M. A., C. A. Gersbach, K. E. Michael, B. G. Keselowsky, and A. J. Garca, "Myoblast proliferation and differentiation on fibronectin-coated self assembled monolayers presenting different surface chemistries.," *Biomaterials*, Vol. 26, pp. 4523–4531, Aug 2005.

35. Ma, Z., Z. Mao, and C. Gao, "Surface modification and property analysis of biomedical polymers used for tissue engineering.," *Colloids Surf B Biointerfaces*, Vol. 60, pp. 137–157, Nov 2007.

36. Di Silvio, L., *Cellular response to biomaterials*, Woodhead Publishing, 2006.

37. Rodrigues, S. N., I. C. Goncalves, M. C. L. Martins, M. A. Barbosa, and B. D. Ratner, "Fibrinogen adsorption, platelet adhesion and activation on mixed hydroxyl-/methyl-terminated self-assembled monolayers.," *Biomaterials*, Vol. 27, pp. 5357–5367, Nov 2006.

38. Wu, G., "Amino acids: metabolism, functions, and nutrition.," *Amino Acids*, Vol. 37, pp. 1–17, May 2009.

39. Haff, R. F., and H. E. Swim, "The amino acid requirements of rabbit fibroblasts, strain rm3-56.," *J Gen Physiol*, Vol. 41, pp. 91–100, Sep 1957.

40. Eagle, H., "The specific amino acid requirements of a mammalian cell (strain l) in tissue culture.," *J Biol Chem*, Vol. 214, pp. 839–852, Jun 1955.

41. Graham, C. A., A. E. Hughes, and N. C. Nevin, "Differences in proteins secreted by human fibroblasts and muscle cells in culture.," *Exp Cell Res*, Vol. 154, pp. 320–325, Sep 1984.

42. Chang, H. I., and Y. Wang, "Cell responses to surface and architecture of tissue engineering scaffolds," *Regen. Med. and Tissue Eng.*, pp. 569–588, 2011.

43. Tamada, Y., and Y. Ikada, "Cell adhesion to plasma-treated polymer surfaces," *Polymer*, Vol. 34, no. 10, pp. 2208 – 2212, 1993.

44. Lee, J. H., H. W. Jung, I. K. Kang, and H. B. Lee, "Cell behaviour on polymer surfaces with different functional groups.," *Biomaterials*, Vol. 15, pp. 705–711, Jul 1994.

45. Lee, N. Y., and B. H. Chung, "Novel poly(dimethylsiloxane) bonding strategy via room temperatureâ "chemical gluing"," *Langmuir*, Vol. 25, no. 6, pp. 3861–3866, 2009.

46. Teixeira, A. I., S. Ilkhanizadeh, J. A. Wigenius, J. K. Duckworth, O. Inganas, and O. Hermanson, "The promotion of neuronal maturation on soft substrates.," *Biomaterials*, Vol. 30, pp. 4567–4572, Sep 2009.

47. Greene, T., *Protective groups in organic synthesis*, Wiley, 1998.

48. Ozturk, M. O., "Preparation and characterization of cartilage mimicked structures," Master's thesis, Bogazici University, 2014.

49. Han, Y., D. Mayer, A. OffenhÃusser, and S. Ingebrandt, "Surface activation of thin silicon oxides by wet cleaning and silanization," *Thin Solid Films*, Vol. 510, no. 1â2, pp. 175 – 180, 2006.

50. Flink, S., F. C. J. M. van Veggel, and D. N. Reinhoudt, "Functionalization of self-assembled monolayers on glass and oxidized silicon wafers by surface reactions," *Journal of Physical Organic Chemistry*, Vol. 14, no. 7, pp. 407–415, 2001.

51. Schmid, F. X., *Biological Macromolecules: UV-visible Spectrophotometry.* John Wiley & Sons, Ltd, 2001.

52. Lobo, A., E. Antunes, M. Palma, C. Pacheco-Soares, V. Trava-Airoldi, and E. Corat, "Biocompatibility of multi-walled carbon nanotubes grown on titanium and silicon surfaces," *Materials Science and Engineering: C*, Vol. 28, no. 4, pp. 532 – 538, 2008. Proceedings of the Symposium on Nanostructured Biological Materials, V Meeting of the Brazilian Materials Research Society (SBPMat).

53. Harnett, E. M., J. Alderman, and T. Wood, "The surface energy of various biomaterials coated with adhesion molecules used in cell culture.," *Colloids Surf B Biointerfaces*, Vol. 55, pp. 90–97, Mar 2007.

54. Cui, N. Y., C. Liu, and W. Yang, "Xps and afm characterization of the self-assembled molecular monolayers of a 3-aminopropyltrimethoxysilane on silicon surface, and effects of substrate pretreatment by uv-irradiation," *Surface and Interface Analysis*, Vol. 43, no. 7, pp. 1082–1088, 2011.

55. Bohmler, J., *Well-controlled and well-described SAMs-based platforms for the study of material-bacteria interactions occuring at the molecular scale.* PhD thesis, Universit de Haute Alsace-Mulhouse, 2012.

56. Yam, C. M., and A. K. Kakkar, "Molecular self-assembly of dihydroxy-terminated molecules via acid-base hydrolytic chemistry on silica surfaces: step-by-step multilayered thin film construction," *Langmuir*, Vol. 15, no. 11, pp. 3807–3815, 1999.

57. Li, Z., W. Han, D. Kozodaev, J. C. Brokken-Zijp, G. de With, and P. C. Thune, "Surface properties of poly(dimethylsiloxane)-based inorganic/organic hybrid materials," *Polymer*, Vol. 47, no. 4, pp. 1150 – 1158, 2006.

58. Schroeder, T., M. Adelt, B. Richter, M. Naschitzki, M. BÃumer, and H.-J. Freund, "Growth of well-ordered silicon dioxide films on mo(112)," *Microelectronics Reliability*, Vol. 40, no. 4â5, pp. 841 – 844, 2000.

59. Senthilkumar, S. T., R. K. Selvan, J. S. Melo, and C. Sanjeeviraja, "High performance solid-state electric double layer capacitor from redox mediated gel polymer electrolyte and renewable tamarind fruit shell derived porous carbon.," *ACS Appl Mater Interfaces*, Vol. 5, pp. 10541–10550, Nov 2013.

60. Miura, A., T. Takei, and N. Kumada, "Low-temperature nitridation of manganese and iron oxides using nanh2 molten salt.," *Inorg Chem*, Vol. 52, pp. 11787–11791, Oct 2013.

61. Zhang, L., A. Chatterjee, M. Ebrahimi, and K. T. Leung, "Hydrogen-bond mediated transitional adlayer of glycine on si(111)7 x 7 at room temperature.," *J Chem Phys*, Vol. 130, p. 121103, Mar 2009.

62. A., V., S. H. R., J. Kohlscheen, S. Rambadt, and G. Erkens, "Oxidation resistance of titanium-aluminium-silicon nitride coatings," *Surface and Coatings Technology*, Vol. 174-175, no. 0, pp. 408 – 415, 2003. Proceedings of the Eight International Conference on Plasma Surface Engineering.

63. Dong, H., K. Chen, D. Wang, W. Li, Z. Ma, J. Xu, and X. Huang, "A new luminescent defect state in low temperature grown amorphous sinxoy thin films," *physica status solidi (c)*, Vol. 7, no. 3-4, pp. 828–831, 2010.

64. Kallury, K. M. R., U. J. Krull, and M. Thompson, "X-ray photoelectron spectroscopy of silica surfaces treated with polyfunctional silanes," *Analytical Chemistry*, Vol. 60, no. 2, pp. 169–172, 1988.

65. Leroy, E., O. M. Kuttel, L. Schlapbach, L. Giraud, and T. Jenny, "Chemical vapor deposition of diamond growth using a chemical precursor," *Applied Physics Letters*, Vol. 73, no. 8, pp. 1050–1052, 1998.

66. Gautam, S., A. K. Dinda, and N. C. Mishra, "Fabrication and characterization of pcl/gelatin composite nanofibrous scaffold for tissue engineering applications by electrospinning method.," *Mater Sci Eng C Mater Biol Appl*, Vol. 33, pp. 1228–1235, Apr 2013.

67. Kim, J. J., L. Duan, T. G. Tu, O. Elie, Y. Kim, N. Mathiyakom, D. Elashoff, and Y. Kim, "Molecular effect of ethanol during neural differentiation of human embryonic stem cells in vitro.," *Genom Data*, Vol. 2, pp. 139–143, Dec 2014.

68. Wei, C., L. Xiaoying, Z. W., and Z. Yi, "Study on si-surface modification with chitosan and cell adhesion," in *Medical Devices and Biosensors, 2008. ISSS-MDBS 2008. 5th International Summer School and Symposium*, 2008.

69. Zhu, X. M., L. K. C. F. Wang Y. X. J., and, S. F. Lee, F. Zhao, D. W. Wang, M. Y. J. Lai, C. Wan, C. H. K. Cheng, and A. T. Anil T Ahuja, "Enhanced cellular uptake of aminosilane-coated superparamagnetic iron oxide nanoparticles in mammalian cell lines," *Int J Nanomedicine*, Vol. 7, pp. 953–964, 2012.

70. Heo, S. C., D. Yoo, M. Choi, and C. Choi, "Remote nh3 plasma passivation on the interface between the remote plasma al2o3 atomic layer deposited and 6h sic substrate," *Journal of Ceramic Processing Research*, Vol. 13, pp. 657–661, 2012.

71. Fan, Y. W., F. Z. Cui, L. N. Chen, Y. Zhai, Q. Xu, and I.-S. Lee, "Adhesion of neural cells on silicon wafer with nano-topographic surface," *Applied Surface Science*, Vol. 187, no. 3-4, pp. 313–318, 2002.

72. Lu, Y., C. Yang, J. Yeh, F. Ho, Y. Ou, C. Chen, M. Lin, and K. Huang, "Guidance of neural regeneration on the biomimetic nanostructured matrix," *International Journal of Pharmaceutics*, Vol. 463, no. 2, pp. 177 – 183, 2014. Improved Wound Dressing: Novel Approaches.

73. Davis, D. H., C. S. Giannoulis, R. W. Johnson, and T. A. Desai, "Immobilization of rgd to $<$ 1 1 1 $>$ silicon surfaces for enhanced cell adhesion and proliferation.," *Biomaterials*, Vol. 23, pp. 4019–4027, Oct 2002.

74. Hsu, C., Y. Wu, W. Lee, L. Li, and J. Lin, "Effects of targeted anticancer medicines on post-cell removal surface morphology of cancer cells cultivated on 3-aminopropyltriethoxysilane surfaces," *Med chem*, Vol. S1, pp. 2165–0444, 2014.

75. Garipcan, B., S. Odabas, G. Demirel, J. Burger, S. S. Nonnenmann, M. Coster, E. M. Gallo, B. Nabet, J. E. Spanier, and E. Piskin, "In vitro biocompatibility of n-type and undoped silicon nanowires," *Advanced Engineering Materials*, Vol. 13, no. 1-2, pp. B3–B9, 2011.

76. Wallat, K., D. Dorr, R. Le Harzic, F. Stracke, D. Sauer, M. Neumeier, A. Kovtun, H. Zimmermann, and M. Epple, "Cellular reactions toward nanostructured silicon surfaces created by laser ablation," *Journal of Laser Applications*, Vol. 24, no. 4, pp. –, 2012.

77. Ma, Z., C. Gao, J. Yuan, G. Y. Ji, J., and J. Shen, "Surface modification of pol-l-lactide by photografting of hydrophilic polymers towards improving its hydrophilicity," *Journal of Applied Polymer Science*, Vol. 85, pp. 2163–2171, 2002.

78. Wei, J., M. Yoshinari, S. Takemoto, a. K. E. Hattori, M., B. Liu, and Y. Oda, "Adhesion of mouse fibroblasts on hexamethyldisiloxane surfaces with wide range of wettability," *Journal of Biomedical Materials Research Part B: Applied Biomaterials*, Vol. 81B, no. 1, pp. 66–75, 2007.

79. Yoshinari, M., K. Matsuzaka, and T. Inoue, "Surface modification by cold-plasma technique for dental implants - bio-functionalization with binding pharmaceuticals," *Japanese Dental Science Review*, Vol. 47, no. 2, pp. 89–101, 2011.

80. Kyte, J., and R. F. Doolittle, "A simple method for displaying the hydropathic character of a protein.," *J Mol Biol*, Vol. 157, pp. 105–132, May 1982.

81. Xu, S. J., F. Z. Cui, X. L. Yu, and X. D. Kong, "Glioma cell line proliferation controlled by different chemical functional groups in vitro," *Frontiers of Materials Science*, Vol. 7, no. 1, pp. 69–75, 2013.

82. Nelson, D. L., and M. Cox, *Lehninger Principles of Biochemistry*, Macmillan Education, 2013.

83. Cui, Y. X., K. M. Shakesheff, X. Chen, and G. Adams, "The role of poly-l-ornithine, poly-l-lysine and extracellular matrix proteins on the proliferation and function of pancreatic insulin-producing beta cells by complex alginate microencapsulation," *European Cells and Materials*, Vol. 10, p. 40, 2005.